



GLOBAL JOURNAL OF RESEARCHES IN ENGINEERING: J
GENERAL ENGINEERING

Volume 25 Issue 1 Version 1.0 Year 2025

Type: Double Blind Peer Reviewed International Research Journal

Publisher: Global Journals

Online ISSN: 2249-4596 & Print ISSN: 0975-5861

Magnetic Resonance Therapy (MRT) and Relativistic Effect of Rotation

By Yin Rui, Yin Ming & Wang Yang

Bei Hang University

Abstract- Epoxide within molecular structures is recognized as hallmarks of potent carcinogenic cells. This paper proposes a novel approach: Magnetic Resonance Therapy (MRT), which selectively eliminates epoxide in cancerous tissues while preserving oxygen in healthy tissues, offering a potentially side-effect-free method for cancer treatment and prevention. The study presents a series of in vitro, in vivo, and clinical experiments to support this innovative therapeutic strategy. The underlying mechanism of MRT is grounded in the principles of relativity for rotational frames, and an experimental validation of this theoretical framework is provided. Furthermore, this research unveils previously undescribed relativistic phenomena, including space-time exchange, critical cylinder effects, strong and sub-strong and weak interactions as well as the source of quantum property and the source of mass as well as dark mas. Due to space constraints, the detailed mechanism of epoxide elimination will be elucidated in a subsequent publication.

Keywords: cancer, epoxide, magnetic resonance therapy, relativity for rotational frames.

GJRE-J Classification: LCC: QC173.96



Strictly as per the compliance and regulations of:



Magnetic Resonance Therapy (MRT) and Relativistic Effect of Rotation

Yin Rui^α, Yin Ming^σ & Wang Yang^ρ

Abstract- Epoxide within molecular structures is recognized as hallmarks of potent carcinogenic cells. This paper proposes a novel approach: Magnetic Resonance Therapy (MRT), which selectively eliminates epoxide in cancerous tissues while preserving oxygen in healthy tissues, offering a potentially side-effect-free method for cancer treatment and prevention. The study presents a series of in vitro, in vivo, and clinical experiments to support this innovative therapeutic strategy. The underlying mechanism of MRT is grounded in the principles of relativity for rotational frames, and an experimental validation of this theoretical framework is provided. Furthermore, this research unveils previously undescribed relativistic phenomena, including space-time exchange, critical cylinder effects, strong and sub-strong and weak interactions as well as the source of quantum property and the source of mass as well as dark mas. Due to space constraints, the detailed mechanism of epoxide elimination will be elucidated in a subsequent publication.

Keywords: cancer, epoxide, magnetic resonance therapy, relativity for rotational frames.

PART 1. THE PRACTICE OF MRT TREATING CANCER

I. INTRODUCTION

It is well known that lots of diseases is caused by oxidation of cell molecules. As pointed by James D. Watson in his book "Molecular Biology of the Gene" (1): "the procarcinogens become into powerful carcinogens, as the epoxide appears in their molecules." An efficient and non-hazardous way to clean epoxide is proposed in this paper. We call it Magnetic Resonance Therapy (MRT). No medicine, no radioactivity, no scalpel, the MRT uses very weak magnetic field (less than 10 Gs) to clean epoxide. Its equipment is consisted of a signal generator (the gray box in Fig. 1) and a group of coils with air core (the white cylinder in Fig. 1). The signal generator produces currents, those flow through the coils to generate both main and RF magnetic fields acting on the lesion. The coils are positioned 20 cm away from the body surface, since the resonance happens beyond that place until 60 cm. The treatment starts when the signal generator is turned on. The standard dosage is three times one-hour per day. The device is very light (the total weight is 2 Kgs only), easy-managed, so that it can be used not only in hospital but also at home. And since it is no-hazard but benefit for body, it can be used to prevent cancer. Every year take MRT a month, even in sleep time, can keep the cancer away all life.



Fig. 1: Equipment and usage

a) Cell and Animal Experiments

i. The Killed Process of Cancer Cells by MRT–Cell Experiment in Vitro

Giving cultured squamous cancer cells MRT and observing the killed process of cells, we find that as MRT has been given for 5 minutes, lots of expanding bubbles bulge on the membrane of cells; as MRT has been given for 10 minutes, all bubbles expand to break, perforations appear at the place covered by bubbles before. The cell is dead currently. Continue MRT, perforations become bigger and bigger, the cell is broken.

Author ^α ^σ ^ρ: Bei Hang University. e-mail: yr195@buaa.edu.cn

ii. Cell Experiment in Vivo

Five days later after inoculating the Ehrlich (liver ascites cancer) line into the abdomen of 20 mice (BALB/c), every mouse grew up ascites including lots of Ehrlich cancer cells. Take 10 of them as experimental group and give them 8 days MRT (90minutes/day). The microscope photo-pictures are shown as Figure 2, where upper left is the cancer cells in control mice, every cell is complete. Upper right are the cells in experimental mice, perforations, overflowing cytoplasm, pieces of broken cells and dissolving into ascites can be observed. Lower left are the blood cells in control mice, lower right are the blood cells in experiment mice. They are no difference, means MRT does not damage blood cells.

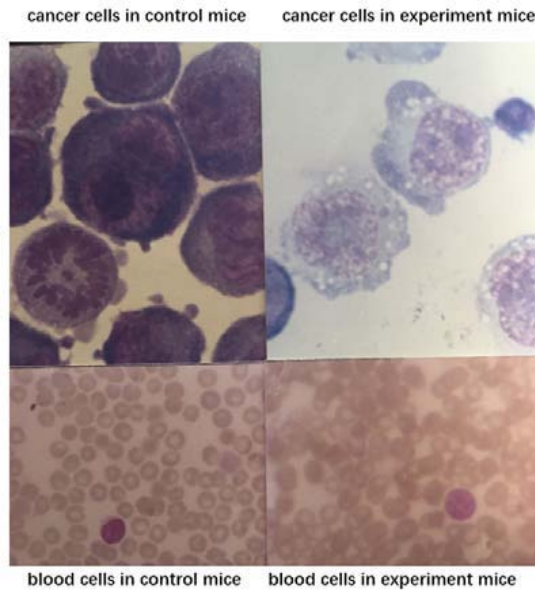


Fig. 2: MRT kill cancer cells but no effect to blood cells

iii. The Efficiency of MRT on Ascitic Hepatoma (Ehrlich) in Mice

Mice were inoculated with Ehrlich line, and significant ascitic growth was observed five days post-inoculation. On the tenth day, efficacy experiments were conducted. Before MRT, a small volume of ascitic fluid was extracted and examined under a microscope for cell count, yielding a concentration of 3.13×10^8 /ml. Magnified images of the cells are shown in Figure 3 (left panel).

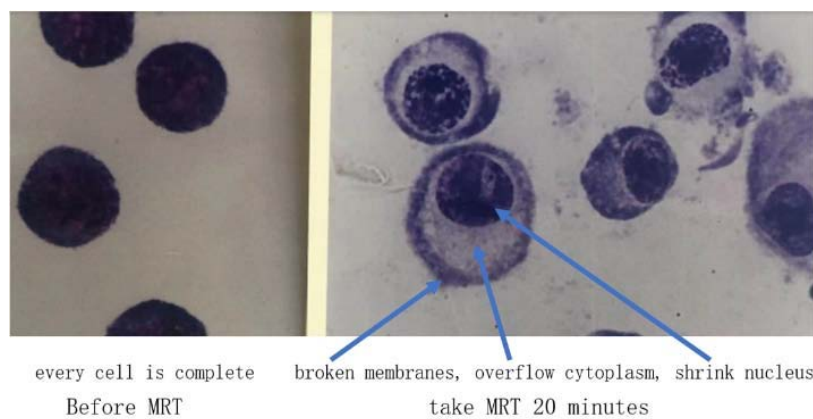


Fig. 3: MRT can kill Ehrlich cancer cell in 20 minutes

After 20 minutes of MRT, another small sample of ascitic fluid was collected for observation. The resulting image is displayed in Figure 3 (the right panel)). It was observed that, prior MRT, the cancer cells appeared intact. However, following 20 minutes of MRT, the cell nuclei exhibited pyknosis, ruptured, and released bubbles, causing perforation (visible as white spots in the images). The cell membranes fragmented, and cytoplasm leakage occurred, displacing membrane debris into a hollow area approximately twice the size of the nucleus. At this stage,

the cells were confirmed to be dead, although complete dissolution into the surrounding fluid required less than an hour

At 1.5 hours MRT, a subsequent ascitic fluid sample was analyzed for cell count, yielding a concentration of 0.117×10^8 /ml. Compared to pre-treatment levels, this indicated a cell kill rate of 96%.

At 5.5 hours post-treatment, another ascitic fluid sample was examined, showing a cell count of 0.094×10^8 /ml. This further confirmed a cell kill rate of 97% relative to pre-treatment levels.

iv. MRT Treated Lewis Lung Cancer in Black Mice With 100% Cure Rate

Four days after inoculating Lewis's lung cancer line, eleven mice of C57BL/6J all grew cancer blocks with the size of about 3mm. Three of them were taken as the control group, four of them were taken as the experimental group with small dose (10 minutes/day), and the other four mice were taken as big dose group (70 minutes/ day). One week later we ended MRT, the cancer blocks in control mice all grew to the size of about 2cm, but the cancer blocks in six experimental mice (four of big dose group and two of small dose group) disappeared. However, there was a tuber in the size of about 1cm for two mice of small dose group. We dissected four mice. The cancer block in control mouse is shown as Figure 4 (the upper middle one), the upper right one is the tuber in the mouse taken small dose. The picture of dissected mouse without cancer block is shown in Figure 4 lower middle, The lower right is the tuber under Electron-Microscope. It is shown that there isn't any cancer embolus in it.

Two weeks later the other two mice of control group dead. However, one month later the tuber in the left mouse of the small dose group naturally disappeared. Nine months later the left five mice were all alive with very good health, and we ended this experiment. Such cure rate (100%) was scarce for animal experiment of cancer.

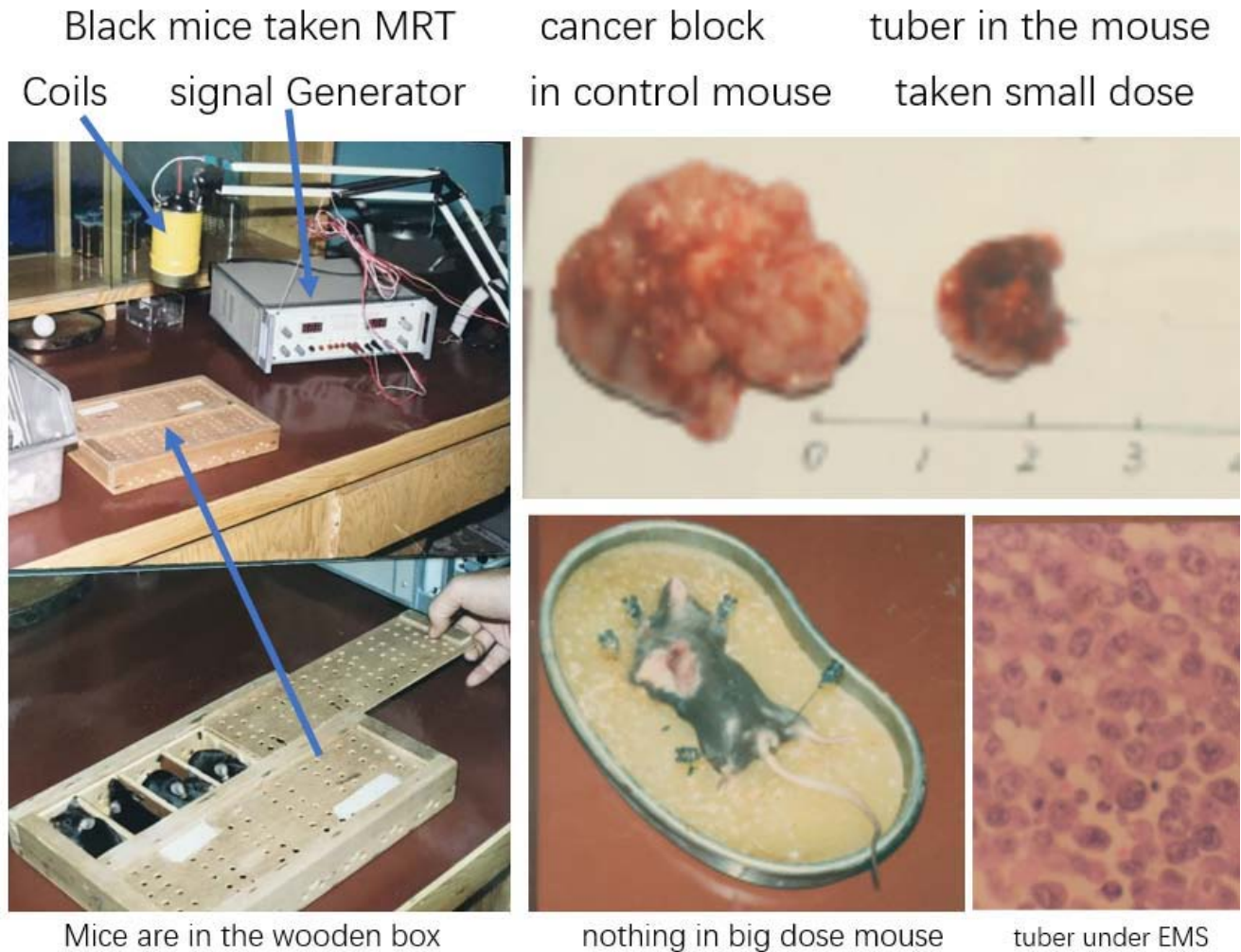


Fig. 4: MRT treated Lewis Lung Cancer in Black Mice

b) *Clinical Experiments*

More than 50 volunteers have taken MRT, Follows are some cases.

MRT treat nasal polyp before MRT

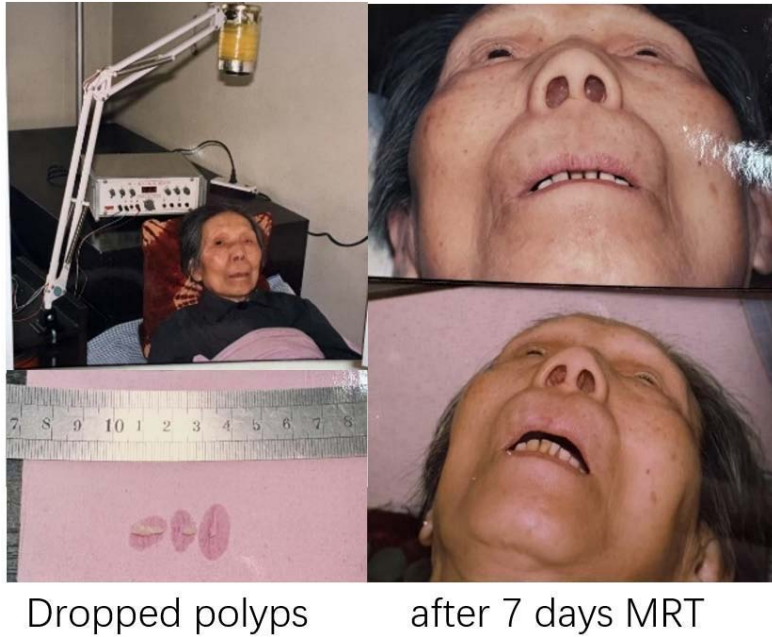


Fig. 5: MRT treat nasal polyp

Case 1: A 93-year-old woman suffered from nasal polyp. The polyps filled both nostrils as shown in Fig.5 (upper right). She took one week MRT (2 hours/day) at her bedroom as shown in Fig.5 (upper left). During the second day's MRT, some polyps with the size about 2mm×8mm were come down on their own, as shown in Fig.5(lower left). After a week MRT the polyps were disappeared completely, as shown in Fig. 5 (lower right).

Case 2: A fifteen years old boy suffered from finger tumor as shown in Fig.6 (a). Two months later after taking MRT three days (3×1hour/day), a piece of hard crust shell was taken off the tumor as shown in Fig.6 (b). After taking another three days MRT, the tumor constricted month by month as shown in Fig.6 (c) (d) (e). Another picture taken at 30 years later is shown on Fig.6. (f).

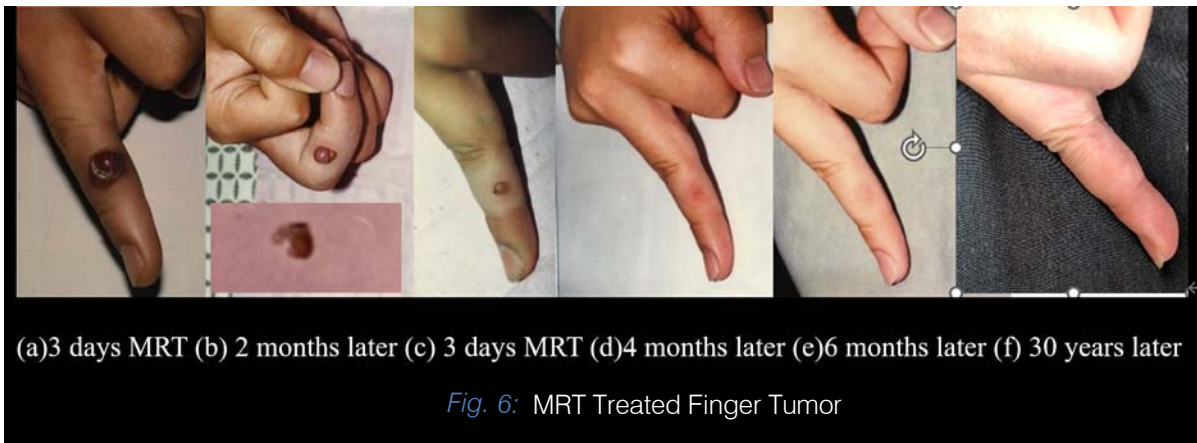


Fig. 6: MRT Treated Finger Tumor

Case 3: The bile duct of an old man was obstructed. Jaundice appeared on his face, hands and body as shown in Fig. 7 (a). He had no appetite and dregs-like stool. He took MRT at home. As the MRT had been given for three hours, a boundary line of jaundice appeared on his forehead, above this line the jaundice disappeared. As the MRT was continuing, the boundary line was going down and down. As the MRT had been given for six hours, the jaundice on his face and hands disappeared. As the MRT had been given for nine hours, the old man said: 'I am so hungry'. We ended that day's MRT and give him a bowl of gruel. Gobbling up the gruel, he said: 'I am hungry too'. His daughter smiled and asked: 'can he eat so much?' We said: 'doesn't matter, give him a diner please'. On the second day his stool became normal. Nevertheless, we gave him another two days MRT again, the picture taken on the third MRT day is shown in Fig. 7 (b).



Fig. 7: MRT Treated Bile Duct Blockage

Case 4: MRT Treat Lung Cancer

A 64-year-old man suffered from lung squamous cancer. The x-ray photo taken on 14.3.1994 is shown as Figure 8(a), where the white elliptic part in upper left lung is the original cancer block. Two weeks later the metastasized cancer blocked the bronchus, air couldn't get into left lung, the left lung atelectasis (so-called white lung) as shown in Figure 8(b). Before MRT, the patient could neither sit nor lay, four or five times of shock happened every day. We gave him a one-week MRT. On the second MRT day he could sit, after the third MRT day he could walk in the garden of the hospital. The x-ray photo taken on the last MRT day is shown as Figure 8(c). His left lung could expand again. 40 days later another x-ray photo was taken and is shown in Fig.8 (d). The situation was much better (Figure 5).

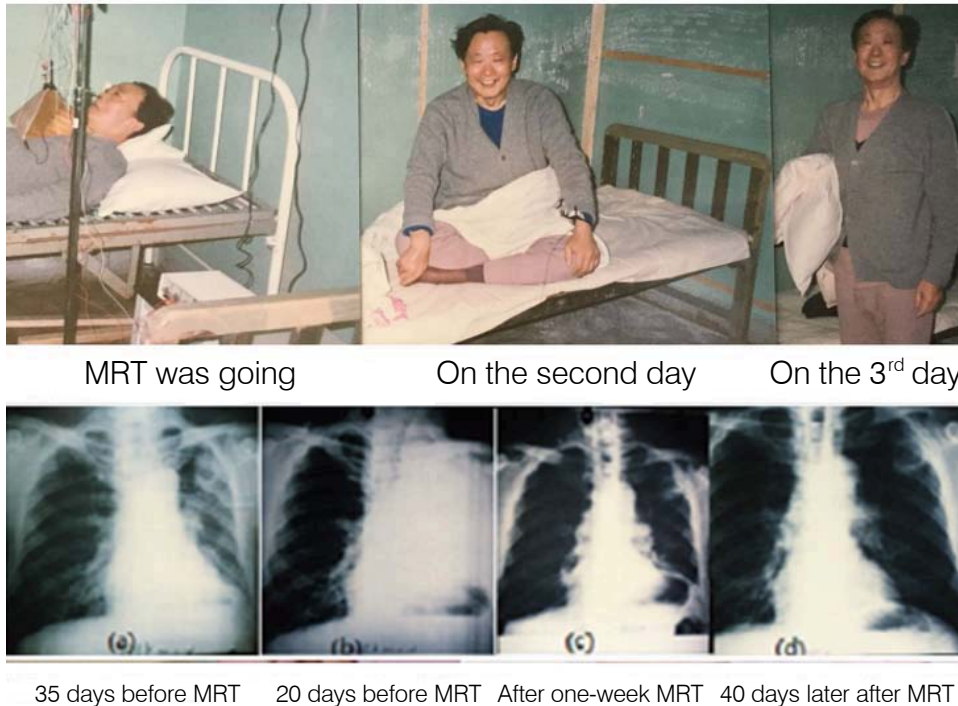


Fig. 8: MRT Treated Lung Cancer

Case 5: MRT Treat Gastric Cancer

Before treatment, the patient's pylorus was completely obstructed by cancer, rendering oral intake impossible, as shown in Figure 9 (upper left). A narrow channel was created using laser treatment, allowing the patient to sustain life by consuming milk and fruit juice. By the fifth day of MRT (3×1hour/day), the patient expelled a significant amount of scabs, part of them displayed in Figure 9 (lower left). Following this, the patient was able to consume stewed beef.

The next day, a gastroscopy was performed. Figure 9 (upper right) presents a video screenshot of the pyloric region, showing that the obstructing cancer around the pylorus had disappeared. Other areas of the gastric wall still exhibited scabs tissue that had not yet shed, as indicated in the gastroscopic video screenshot in Figure 9 (lower right). The image reveals that all areas infiltrated by the tumor had formed scabs, while the uninvolved gastric wall remained its original white color. This indicates that MRT not only avoids damage to normal tissue but also ensures comprehensive targeting of pathological tissue.

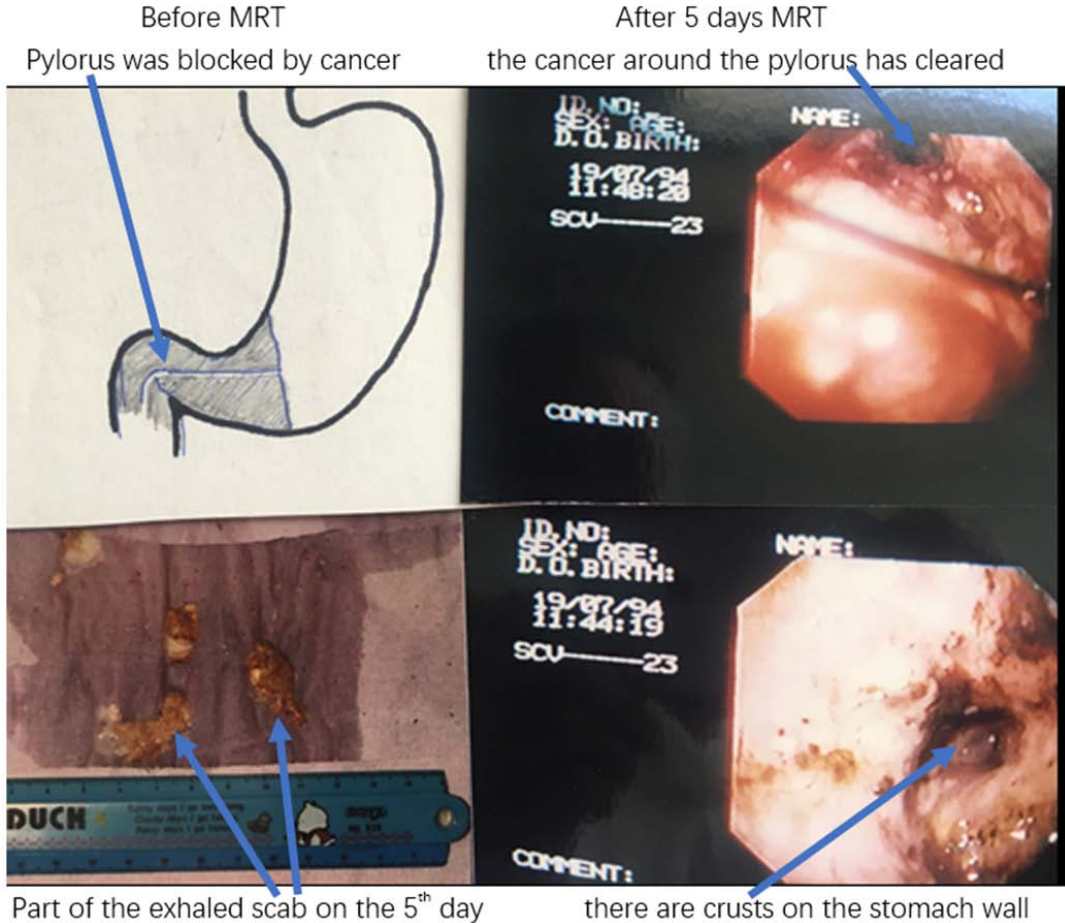


Fig. 9: 5 Days MRT (3hours/day) Cure the Pylorus Cancer

It should be noted that some gastric cancer patients, instead of vomiting necrotic tissue after 4–5 days of treatment, expelled it through defecation, like patients with colorectal cancer.

Above cases show that one or two weeks MRT can cure the cancer with small size. But the big size cancer should take MRT for long time. In this case, MRT can be taken at home and self-service by patients without the help of doctor. Follows are some cases.

Case 6: MRT Treat Lower Jawbone Cancer

A 78 years old woman suffered from lower jawbone cancer, and metastasized. She couldn't eat and sleep. She took MRT at home. The dose was 4×40 minutes/day. Since taking MRT, she could go to sleep every night, because the pain relaxed. Fig. 10 (a) and (b) are the pictures taken before MRT, (c) and (d) are those taken after one month MRT. Comparing them, we see that the cheek swollen disappeared, large area of cancer-ulcer with liquid oozed on chin healed up.



Fig. 10: MRT Treated Lower Jawbone Cancer

Case 7: MRT Treat Breast Small Cell Cancer

At the beginning the size of cancer block was $14\text{cm} \times 12\text{cm}$ as shown in Fig.11. After one-month MRT (3×1 hour/day), the mass in the upper left region disappeared, while the middle portion was charred and necrotic with a cavity being formed as shown in Fig.11. After one year MRT, the cancer tissue carbonized and necrotized into cavities as shown in Fig.11. But the skin around the cancer was without any change, although it suffered one-year MRT as well. This means the MRT can only kill cancer and no affect to normal tissue.



Fig. 11: MRT Treated Breast Small Cell Cancer

Case 8: MRT Treat Prostate Cancer

A 86-year-old man has suffered from prostate cancer for several years. His PSA was 100 ↑ (below 4 normal) on 25.5.2020. The PET-CT photo taken on 2020.6.5 is shown as Fig. 12, where every black point in bone was the cancer metastasis. Since 2020.7.19 he had taken MRT at home (3×1hour/day). After 5 months MRT the PSA was decreased to 2.1, then stop MRT. However, the PSA was still decreased, two months later decreased to 1.1, then increased, five months later increased to 1.89. Then started MRT again, one month later PSA decreased to 0.431. The PET-CT photo taken in September of 2021 is shown in Fig.12. In terms of this photo, we know lots of bone metastasis disappeared.

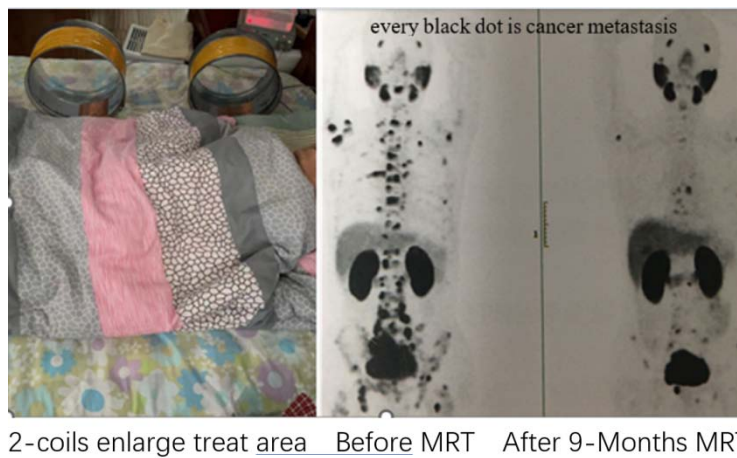


Fig. 12: MRT Treated Prostate Cancer

c) *Prevention and Early-Treatment of Cancer*

MRT can be used not only to treat cancer but also to prevent cancer. Following is an example.

Case 9: A 43-year-old female teacher was tested squamous cancer cells in white deposits on her tongue in 1994. The doctor suggested her to cut part of tongue. She was a teacher; without a complete tongue how could she give lecture? She asked us for help. We gave her one-week MRT (90 minutes/day) at the very beginning, then 3 months MRT (60 minutes per week). Now, 30 years is over, she fulfilled work and retired with wonderful health.

Tumor markers in the blood have exceeded the standard before cancer forms solid tumors. This is the best time for early treatment. MRT can be used as “pre-cancer” treatment, since its device is tiny, its operation is simple, it has no side effect, and it can be used at any place (home, office, class, etc.). Generally, 2 or 3 months later after 3 weeks MRT(3×40 minutes/day) the positive tumor marker can become negative. Following is an example:

Case 10: A 79-year-old academician in physical examination on 2014.12.29 was found that his Squamous Cell Carcinoma (SCC) cell antigen was 12.9 (below 1.5 normal). The doctor in no way helped him, only allowed him to take another test after 3 months. He asked us for help and took 20 days MRT at home from 2015.1.10 to 2015.1.30. After that 3 examinations were performed on 2015.1.30, 2015.3.13, and 2015.4.10. The results were: 8.1;4.1 and 0.8. Then in 2016,17,18,19 every year he takes one-month MRT. Till now, ten years have been over, his SCC has always been in the normal region.

The essence of MRT is deoxidation, It not only no hazard but benefit to body. Put the device on the bed and turn on it before going to sleep and turn it off after waking up. Doing it like this one month per year can keep cancer away all life.

d) *MRT treat cardio- and brain-vascular diseases*

MRT can be used to treat cardio- and brain-vascular diseases because they are caused by oxidation of cell molecules. Now let us give some cases.

Case 11: 67 years old women suffered from cerebral hemorrhage, after emergency operation, she kept life but left wet brain as shown in Figure 13 (left), so that she couldn't walk, eat and speak. We gave her three months MRT (3×40 minutes/day). After one-month MRT, she could eat meal with chopsticks, go to bathroom freely, and talk fluently. However, there was blood in her brain as shown in Figure 13 (middle). After three months MRT the blood in her brain disappeared. The place where the blood occupied before became empty as shown in Figure 13 (right).

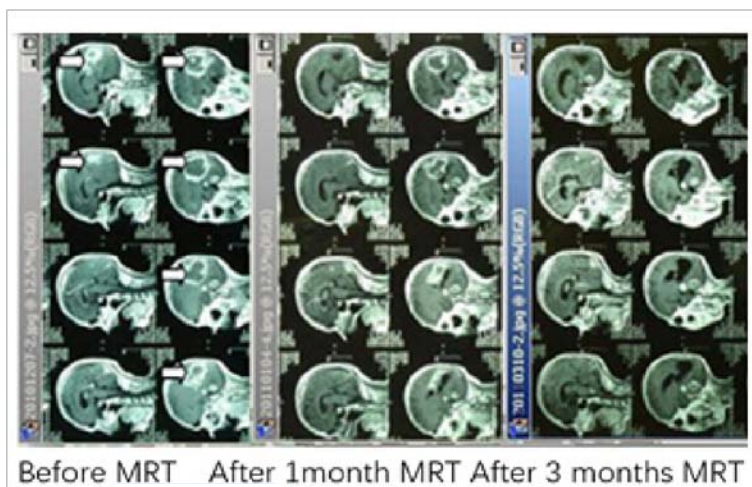


Fig. 13: MRT treated cerebral hemorrhage



Fig.14 arteria peroneal blocked

Case 12: The arteria peroneal of a 76-year-old man was blocked as shown in Fig. 14. Doctor suggested him to take an operation after the other two vascular being blocked. He asked us to help. We gave him 40 minutes MRT in the afternoon. At that night, as he was sleeping, he felt terrible itch on shank and foot. And he thought why there were so many mosquitoes this night. Suddenly, he understood that not mosquito but the blood was flowing though the shank and foot. Nevertheless, we gave him two days MRT again (40 minutes/day) and suggested him to take another test. He said: “no need, I can feel it is very well”. Now he is 90 years old and can walk 500m by push a wheelchair.

Case 13: Prevention of cerebral infarction: One of A 63-year-old man had a precursor to cerebral infarction: dropping chopsticks as eating and speaking incoherently. After 3 days of MRT, the precursor symptoms disappeared. Seven years have passed, and during these years, he has taken MRT regularly, and the condition has been good.

Case 14: Treatment of atrial fibrillation: One of a retired professor had two atrial fibrillations in 2014 and 15, and each time he had two days and three nights of continuous infusion in hospital before returning to normal. In 2016, when he had another attack, he happened to have an MRT device at home, and after one hour of treatment, he returned to normal.

No need for more cases, the efficiency of MRT has been exhibited. Now let us turn to the mechanism of MRT, that is based on Relativistic Effect of Rotation (RER), which was proposed by us in references [2-4]. Since lots of natural laws revealed by RER are unknown for modern physics, we have to give an experiment to prove it first [5].

PART 2. THE RELATIVISTIC EFFECT OF ROTATION

a) Experimental observation of relativistic effect of rotation

It is well known that the tangential velocity v , angular velocity ω , and the radial distance r have the relation of $v=r\omega$. Therefore, any rotation has a corresponding radial distance r_c where v reaches the speed of light c : $r_c=c/\omega$. We call r_c critical radius. All points with their radial distance being r_c form a cylindrical surface called critical cylinder. Almost everyone believes that the tangential velocity Outside Critical Cylinder (OCC) will surpass the speed of light, and superluminal is impossible, so they give-up researching it. However, our experiments demonstrate that there is observable physical phenomena in OCC, which are opposite to those Inside Critical Cylinder (ICC). Now let us show the experiments

The experiment setup and result

A helical electrode is connected to the negative output terminal of a DC high voltage generator (HVG). When the HVG is turned on, an abundance of free electrons will accumulate on the electrode. The electrode is affixed to a resin plate, which is secured in a plastic dish. The two ends of two U-type ferrite cores clamp the electrode, resin plate and the plastic dish together, while the other two ends are inserted into the exciting coils, as shown in Fig. 1. A square wave current generator (SWCG) feeds the coils, producing a magnetic field that is transferred to the electrode via two ferrite cores, causing the free electrons on the electrode to precession. The angular velocity of precession is given by Larmor equation: $\omega=\gamma B$. for electron, its gyromagnetic ratio $\gamma=2.6667 \times 10^{10}$ (Hz/Tesla), as $B=0.12$ Tesla, the precession angular velocity is $\omega=2.01 \times 10^{10}$ (r/s), the corresponding critical radius r_c is 1.492 cm, approximately 1.5 cm. A 20% carbon ink containing a high concentration of anionic surfactants (negatively charged ions) was utilized as the test charge. To begin, warm water is added to the plastic dish, and a small quantity of ink is injected 1 to 1.3 cm to the right of the electrode.

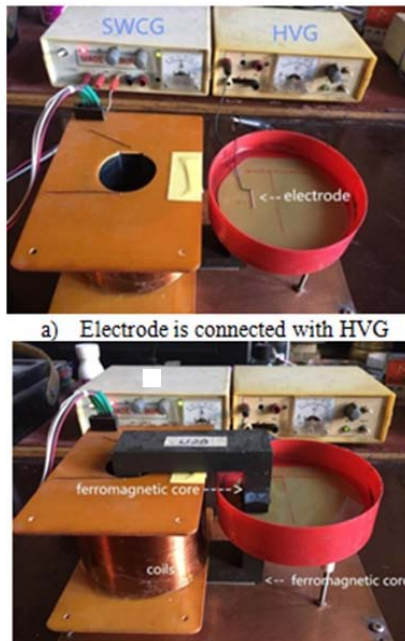


Fig. 1: The experimental device

The HVG is then turned on to recharge electrons on the electrode. The ink is repelled by the electrons, showing a distinct rightward shift as illustrated in the 4 sequential screenshots from the video presented in Figure 2(b).

Once the ink's right edge is repelled to the black mark indicating the resin board's center, the SWCG is activated to induce precession of the electrons. Subsequently, the ink in left side of 1.5cm continues being repelled rightward, whereas the ink in right side of 1.5cm begins being attracted leftward by the precession electrons. Figure 2(c) sequentially presents 6 screenshots from the experimental video depicting this stage of the precession.

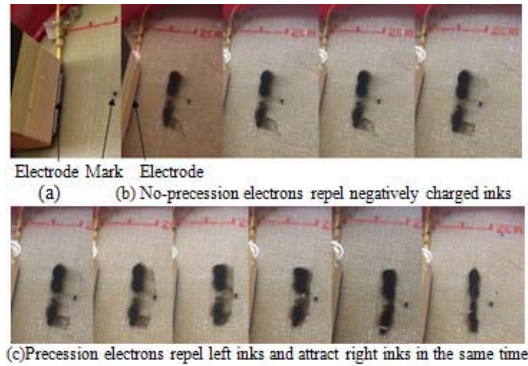
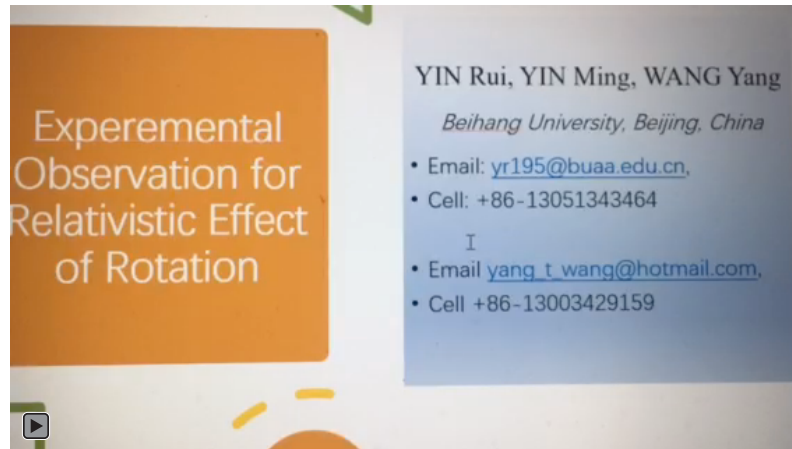


Fig. 2: Ten screenshots of an experimental video

Following is the experiment video: <https://youtu.be/c6YwqfB1KvM>



This experimental result demonstrates following conclusions

1. The electric force of precession electrons exists in OCC but has the opposite direction to that in ICC. This is a relativistic effect of rotation; we term the Critical Cylinder Effect (CCE). CCE reveals the incompleteness of Coulomb's law and Newton's gravitational law.
2. The observed critical radius indicates the precession of electrons possesses definite axis and constant angular velocity, so it is real rotation. Since only a rotating object can create precession when an external torque is applied, the spin of electron must be real rotation, contrary to claims of "not being a real rotation." in quantum spin theory.
3. Furthermore, quantum field theory believes that the electric force is transferred by virtual photons, which means that electrons emit virtual photons and hit the negative ions, causing the momentum change of the negative ions; the rate of momentum change is the force on the negative ions. However, this fails to explain why photon exchanges would exert opposing forces on either side of the critical radius. Electrical force must interact with a medium rotating in sync, i.e. its electric field but not virtual photons. In fact, the strong and weak force, and gravity are the relativistic effect of electromagnetic force, that we will explain in following.
4. There is field force in OCC means the tangential velocity of electric field of the precessing electron does not exceed the speed of light. In OCC, the relation between v and of fixed axis rotation is no longer $v=r\omega$, but $v=c2/(r\omega)$, which has not yet been known for modern physics. Reference (4) has seriously proved it. Now let us give the simple theoretic proof.

b) Space-Time exchange and Tangential Velocity of a Rotation

Suppose frame A' is rotating with a constant angular velocity ω about a fixed axis z (z') relative to frame A . It is well known that substituting the local reference frames of event point P for inertial frames, i.e. substituting (ds, dp, dz, dt) for (x, y, z, t) and $\rho\omega$ for v into the (inverse) Lorentz transformation of inertial frames (1), the (inverse) Lorentz transformation for rotational frames can be got for the area of Inside Critical Cylinder (ICC) as shown in (2):

$$\left\{ \begin{array}{l} x = \gamma(x' + vt') \\ y = y' \\ z = z' \\ t = \gamma(t' + \frac{v}{c^2}x') \end{array} \right. \quad (1) \quad \left\{ \begin{array}{l} ds = \gamma(ds' + \rho\omega dt') \\ d\rho = d\rho' \\ dz = dz' \\ dt = \gamma(dt' + \frac{\rho\omega}{c^2}ds') \end{array} \right. \quad (2)$$

Now, let's extend them to OCC. The $d\rho = d\rho'$ and $dz = dz'$ are kept for OCC too, so we only consider the first and last equations of (2) only. They are:

$$\left\{ \begin{array}{l} ds = \gamma(ds' + \rho\omega dt') \\ dt = \gamma(dt' + \frac{\rho\omega}{c^2}ds') \end{array} \right. \quad (3)$$

Note:

$$\gamma = \frac{1}{\sqrt{1 - \rho^2\omega^2/c^2}} = \frac{ic}{\rho\omega} \frac{\pm 1}{\sqrt{1 - c^2/(\rho^2\omega^2)}} = \frac{ic}{\rho\omega} \gamma' \quad (4)$$

Where,

$$\gamma' = \frac{\pm 1}{\sqrt{1 - c^2/(\rho^2\omega^2)}} = \frac{\pm 1}{\sqrt{1 - \rho_c^2/\rho^2}}, \quad i = \sqrt{-1} \quad (5)$$

Thus, equation (3) can be written as:

$$\left\{ \begin{array}{l} ds = \gamma ds' + \gamma' ic dt' \\ ic dt = \gamma ic dt' - \gamma' ds' \end{array} \right. \quad (6)$$

And can be denoted in complex form: $[ds, ic dt] = [(\gamma ds' + \gamma' ic dt'), (\gamma ic dt' - \gamma' ds')] \quad (7)$

For ICC, γ is real, γ' is imaginary, $(\gamma ds' + \gamma' ic dt')$ is real, $(\gamma ic dt' - \gamma' ds')$ is imaginary. Taken the real and imaginary parts of the two sides of (7) to be equal respectively, equation (6), i.e. eq. (3) can be got.

For OCC, γ is imaginary, γ' is real, $(\gamma ds' + \gamma' ic dt')$ is imaginary, $(\gamma ic dt' - \gamma' ds')$ is real. Taken the real and imaginary parts to be equal respectively again, following equation (8) can be got.

$$\left\{ \begin{array}{l} ds = \overleftarrow{ICC} = \gamma ds' + \gamma' ic dt' = \overrightarrow{OCC} = ic dt \\ ic dt = \overleftarrow{ICC} = \gamma ic dt' - \gamma' ds' = \overrightarrow{OCC} = ds \end{array} \right. \quad (8)$$

We call this natural law space-time exchange. which has not been recognized by academics till now, It means the space in frame A' will become to space in ICC but to time in OCC of frame A. And the time in frame A' will become to time in ICC but to space in OCC of frame A.

As the event point is fixed at frame A', i. e. $ds' = 0$, these equations become to:

$$\left\{ \begin{array}{l} ds \overleftarrow{ICC} = \gamma' ic dt' = \overrightarrow{OCC} \rightarrow ic dt \\ ic dt \overleftarrow{ICC} = \gamma ic dt' = \overrightarrow{OCC} \rightarrow ds \end{array} \right.$$

The tangential velocity of this fixed point of A' relative to frame A is:

in ICC:
$$\frac{ds}{dt} = \frac{\gamma' ic dt'}{\gamma dt'} = \frac{\gamma' ic}{\gamma' ic / (\rho \omega)} = \rho \omega = c \rho / \rho_c,$$

in OCC:
$$\frac{ds}{dt} = \frac{\gamma ic dt'}{\gamma' dt'} = \frac{\pm |\gamma'| ic}{\gamma' (\rho \omega)} ic = \begin{cases} c^2 / (\rho \omega) = c \rho_c / \rho & \gamma' = -|\gamma'| \sqrt{1 - \rho^2 / \rho_c^2} \\ -c^2 / (\rho \omega) = -c \rho_c / \rho & \gamma' = |\gamma'| \sqrt{1 - \rho^2 / \rho_c^2} \end{cases}$$

Both ICC and OCC the direction of rotation must be same, so only $c^2 / (\rho \omega) = c \rho_c / \rho$ is the true tangential velocity at OCC. That means γ' must take its minus root.

100 years ago Stern and Gerlach found the electron was spinning, Ulenbeck and Goldsmith proposed that the angular momentum of electron's spin was $L = \pm \hbar / 2$. Then, Lorentz pointed out: if $L = \hbar / 2$, ω should be 10^{26} r/s, then at $\rho = 10^{-14}$ m., the tangential velocity would be $v = \rho \omega = 10^{12}$ m/s, which was 10^4 times of light speed, that was impossible.

Several scientists measured the tangential velocity of electron's spin at the radial distance near $\rho = 10^{-14}$ m, and get the results in the level of 10^4 (m/s), which was one ten-thousandth of light speed only: $v \approx c / 10^4$. In terms of these measured results they believed the angular velocity to be $\omega = v / \rho \approx 10^{18}$ r/s, which was far less than 10^{26} r/s, that can create $L = \pm \hbar / 2$.

So, till now the Quantum Mechanics has thought: the spin of charged particle is not rotation, and the angular momentum doesn't come from rotation but intrinsic.

However, according to our equation: $v = c^2 / (\rho \omega) = c \rho_c / \rho$ i.e.: $c \rho_c = v \rho / c$, as $\rho = 10^{-14}$ m, $v = c / 10^4$ means $\rho_c = 10^{-18}$ m, $\omega = c / \rho_c = 3 \times 10^{26}$ r/s, that can just create $L = \hbar / 2$. On the other hand, only rotational body can create precession as it suffered from external force. Our experiment proves the electron's precession is real rotation, so its spin must be real rotation too. Denying spin to be rotation, unknown the relativistic effect of rotation, quantum spin theory cannot touch the essence of particle world. This is the reason, why the research about particle physics no achievement during last century. Both six quarks model and super string theory cannot introduce the research go ahead. It's the time to correct it.

c) Unification Form of Lorentz Transformations for Rotational Frames

Now we know Outside Critical Cylinder the tangential velocity of a rotation is $v = c^2 / (\rho \omega) = c \rho_c / \rho$,

$1 - v^2 / c^2 = 1 - \frac{c^2}{\rho^2 \omega^2} = 1 - \frac{\rho_c^2}{\rho^2}$, so the Lorentz factor in OCC is:

$$-|\gamma'| = -(1 - c^2 / \rho^2 \omega^2)^{-1/2} = -(1 - \rho_c^2 / \rho^2)^{-1/2}$$

Thus, let
$$v(\rho) = \begin{cases} c \rho / \rho_c & \rho < \rho_c \\ c \rho_c / \rho & \rho > \rho_c \end{cases} \quad \gamma(\rho) = \begin{cases} (1 - \rho^2 / \rho_c^2)^{-1/2} & \rho < \rho_c \\ -(1 - \rho_c^2 / \rho^2)^{-1/2} & \rho > \rho_c \end{cases}$$

The Lorentz transformations for both ICC and OCC can be uniformly denoted as follows:

$$\begin{cases} ds = \gamma(\rho)(ds' + v(\rho) dt') \\ d\rho = d\rho' \\ dz = dz' \\ dt = \gamma(\rho)(dt' + \frac{v(\rho)}{c^2} ds') \end{cases}$$

In terms of this equation, we can get the transformations of mass (m), energy (w), tangential momentum (p_s), radial force (F_ρ), axial force (F_z) and their resultant (F_R) as follows:

$$m = \gamma(\rho)m'[1 + u_s'v(\rho)/c^2];$$

$$w = \gamma(\rho)(w' + v(\rho)p_s'); \quad p_s = \gamma(\rho)(p_s' + v(\rho)E'/c^2);$$

$$F_{\rho/z/R} = \frac{F'_{\rho/z/R}}{\gamma(\rho)[1 + u_s'v(\rho)/c^2]} = \gamma(\rho)F'_{\rho/z/R}[1 - u_sv(\rho)/c^2]$$

At OCC $\gamma(\rho)$ taken minus root, so the mass, energy, tangential momentum and force have opposite sign against those at ICC. We call it Critical Cylinder Effect (CCE). The experiment given above proves the radial force in OCC is opposite against that in ICC. That means the relativistic effects of rotation, proposed by us, is correct.

On the other hand, the force transformations given above, related to u_s , which is the tangential component of the acceptor charge's velocity relative to the doner charge's spin. Even if the acceptor charge's velocity is fixed, the u_s is different for different spin axis direction of doner charge. So that the force is related to the direction of spin axis of the doner charge. Different spin axis direction creates different force, the movement of acceptor is different. This is the source of uncertainty in Quantum Mechanics.



PART 3. HOW DOES STRONG INTERACTION CREATE BETWEEN PROTONS

a) *Explanation of Experimental phenomenon*

i. *Before magnetic field being excited*

The electron is only spinning with critical radius of: $\rho_{ce} \approx 10^{-18}m$. Take lab as reference frame A, relative to A take the spin of an electron as A'. In A' this electron is really at rest. The force exerted by this electron upon the anion of ink is the true electrostatic force F_R' . Transform F_R' into lab frame A by the force transformation, we get the force acted by electron on the anion of ink in lab frame:

$$F_R = \gamma_s(R)F_R'[1 - u_s v_s(R)/c^2]$$

In our experiment: $u_s=0$; and $R \approx 10^{-2}m$, $\rho_{ce} \approx 10^{-18}m$, $\gamma_s(R) = -(1 - (\rho_{ce}/R)^2)^{-1/2} = -1$. Thus: $F_R = -F_R'$.

In terms of Coulomb's experiment: $F_R = k(-e)(-q)/R^2 = keq/R^2$ where $-q$ is the charge of anion. So $F_R' = -keq/R^2$,

In general, if the spinning charge is q , the test charge is q_t , the real electrostatic force in the spinning frame of q is: $F_R' = -kqq_t/R^2$

It means the real rest charge attracts the charge with the same sign, which is opposite against the Coulomb's law. And as $u_s=0$ the force in lab frame is: $F_R = \gamma(R)F_R'$, i.e.

$$F_R / F_R' = \gamma(R) = \begin{cases} [1 - (R/\rho_c)^2]^{-1/2} & R < \rho_c \\ -[1 - (\rho_c/R)^2]^{-1/2} & R > \rho_c \end{cases}$$

We call it the first kind of CCE, as shown in Fig. 3.1(left). It means as R is changed across the critical radius, the force not only change direction but also approach to infinity. This is the source of so-called strong interaction. The strong interaction of protons appears at the level of $10^{-15}m$ (femto meter: fm), so the critical radius of proton's spin is on the level of fm, we take it is $1fm = 1 \times 10^{-15}m$ to discuss.

More general, if $u_s \neq 0$, $F_R = \gamma_s(R)F_R' - \gamma_s(R)F_R' u_s v_s(R)/c^2 = F_e + F_m =$ electric force + magnetic force.

So, the electrical field of a spinning charge q in lab frame is: $E_s = -\gamma_s(R)kq/R^2$

And the magnetic field of a spinning charge q in lab frame is:

$$B_s = \gamma_s(R)[kq/R^2][v_s(R)/c^2] = q\gamma_s(R)v_s(R)\mu_0/(4\pi R^2)$$

For proton $q = +e = 1.602 \times 10^{-19}C$, its spin magnetic field distribution along radial $R = \rho$ is given in table 1

Table 3.1: The distribution of $\gamma(\rho)$ and spin magnetic field B of proton

$R = \rho =$	$0.9\rho_c$	$0.999\rho_c$	$\rho_c = 10^{-15}m$	$1.001\rho_c$	$1.1\rho_c$	$10^{-9}m (nm)$
$\gamma(\rho) =$	2.3	22.3	$\pm \infty$	-22.4	-2.4	-1
$B(T) =$	0.12×10^{14}	1.07×10^{14}	$\pm \infty$	-1.08×10^{14}	-0.087×10^{14}	-4.8×10^{-7}

And the direction of both electrical and magnetic field E and B are given in Fig. 3.1(right)

Thus, we know the direction of both electric field and magnetic field of spinning charged particle in OCC is opposite against that in ICC. So, as put this particle in an external magnetic field B , after longitudinal relaxation, the external magnetic field can coincide with either the spin magnetic field in OCC or that in ICC. This is why they define spin quantum number to be $s = \pm 1/2$ in quantum mechanics. And we know that how roughly it is to describe the spin magnetic property of proton by magnetic moment.

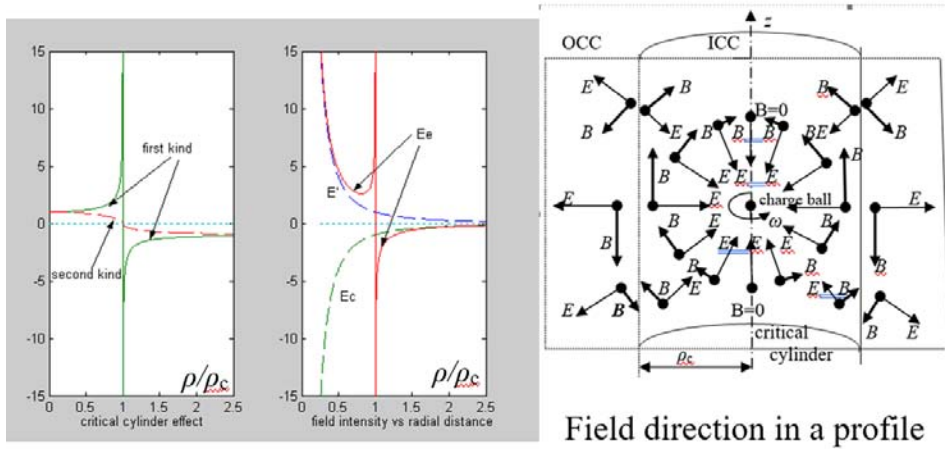


Fig. 3.1: Strength and direction distribution of spinning proton's field

ii. As the magnetic field has been excited

In this case, every electron has two rotations: spin in the angular velocity ω_s and precession with angular velocity of $\omega_m = \gamma B$. Take lab frame as A, the precession of an electron as A', then relative to A' take its spin as A'', then in A'' the force acted on anion of ink by the electron is the real electrostatic force: $F_R'' = -keq / R^2$. Transform F_R'' into A' we have:

$$F_R' = \gamma_s(R) F_R'' [1 - u_s' v_s(R) / c^2] \tag{3.1}$$

Note that both ω_s and ω_m are relative to lab frame A, so the angular velocity of A'' relative to A' is: $\omega_s' = \omega_s - \omega_m$ i.e. $c/\rho_c' = c/\rho_c - c/r_c$, i.e. : $\rho_c' = \rho_c / (r_c - \rho_c)$, so that in equation

$$\gamma_s(R) = \begin{cases} [1 - (R/\rho_c')^2]^{-1/2} & R < \rho_c' \approx 10^{-18} m \\ -[1 - (\rho_c'/R)^2]^{-1/2} & R > \rho_c' \approx 10^{-18} m \end{cases}$$

$$v_s(R) = \begin{cases} cR/\rho_c' & R < \rho_c' \\ c\rho_c'/R & R > \rho_c' \end{cases}$$

Then, transform F_R' into A we have:

$$F_R = \gamma_s(R) \gamma_m(R) F_R'' [1 - u_s' v_s(R) / c^2] [1 - u_m v_m(R) / c^2]$$

In our experiment $u_m = 0$, $(0,5cm < R < 2cm) \gg \rho_c = 10^{-18}m$. $v_s(R) = c(\rho_c / R) \approx 0$, we have:

$$F_R = \gamma_s(R) \gamma_m(R) F_R''$$

Where:

$$\gamma_m(R) = \begin{cases} [1 - (R/r_c)^2]^{-1/2} & R < r_c = 1.5cm \\ -[1 - (r_c / R)^2]^{-1/2} & R > r_c = 1.5cm \end{cases}$$

So, for $R < \rho_c = 10^{-18}m$, F_R is attraction; for $\rho_c < R < r_c$, F_R is repulsion; for $R > r_c$, F_R is attraction, which we have observed in our experiment.

b) *The strong interaction between two protons*

Just like we can think the mass of earth is concentrated in its center, as we discuss the gravity of a body outside the earth, we can think the charge of proton is uniformly distributed in a ball with radius of $b=0.9194fm$, as we discuss the interaction between protons. We will give the detail in part 5 of this paper. Sometimes, for simple, we think the radius of charge ball is $1fm$.

For the two protons system, every proton is spinning with critical radius of ρ_c , that creates spin magnetic field B_s , which makes the other proton precession with critical radius of r_c , that creates precession magnetic field B_m . As the spin and precession axis of every proton are coincide, and anti-parallel to the axes of the other proton, and the distance (R) between two protons is greater than both ρ_c and $2r_c$, the two proton will attract to each other Take lab as A, spin of p_1 as A' , relative to A' take precession of P_1 as A'' . The force exerted on p_2 by p_1 in frame A'' is real electrostatic force $F_R'' = -ke^2/R^2$. Transform it to A' and then to A, we get the force in lab frame as follows

$$F_R = F_R'' \gamma_s(R)(1 - v_s(R)u_s/c^2) \gamma_m(R)(1 - v_m(R)u_m'/c^2) \tag{3.2}$$

Where: u_s is the tangential component of the P_2 's velocity relative to the spin of P_1 in lab frame A
 u_m' is the tangential component of the P_2 's velocity relative to the magnetic precession of P_1 in spin frame A'

$$\begin{aligned} \gamma_s(R) &= -[1 - (\rho_c/R)^2]^{-1/2}, \quad v_s(R) = c(\rho_c/R) \\ \gamma_m(R) &= -[1 - (r_c'/R)^2]^{-1/2} \\ v_m(R) &= c(r_c'/R), \quad r_c' = r_c \rho_c / (\rho_c - r_c) \end{aligned} \tag{3.3}$$

For keeping two protons attract to each other, R must be greater than both ρ_c and r_c' , this means R must be greater than $2r_c$ (accurately $r_c < 0.5002fm$). If $r_c > 0.5003fm$, then $r_c' > R$, the two protons will repel to each other, the two protons system can not exist.

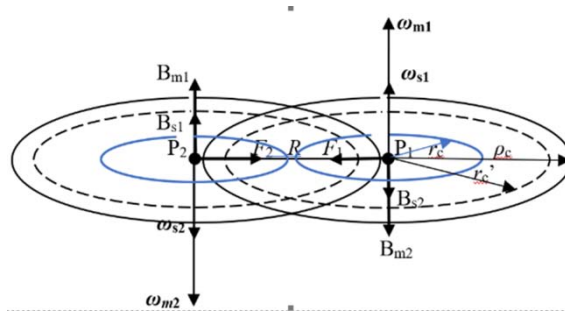


Fig. 3.2: Strong interaction between two protons

In terms of Eq. (3.2), we can get the spin and precession magnetic fields at $\rho=r=R$ as follows:

$$\begin{aligned} B_s &= e[\gamma_m(R)\gamma_s(R)]v_s(R)\mu_0/(4\pi R^2) \\ B_m &= e[\gamma_m(R)\gamma_s(R)]v_m(R)\mu_0/(4\pi R^2) \end{aligned}$$

At the stable state, longitudinal relaxation ended, the spin and precession axes are almost coincided for every proton, and are anti-parallel to the axes of the other proton, as shown in Fig. 3.1. In this case the magnetic field passing through every proton is:

$$B = (B_m + B_s) = e\gamma_m(r)\gamma_s(\rho)[v_s(\rho) + v_m(r)]\mu_0 / (4\pi R^2). \tag{3.4}$$

In terms of Larmor equation: $\omega_m = -2\pi\gamma_p B$, where minus sign means the direction of ω_m is opposite against the direction of passing magnetic field B , we can get the angular velocity of proton's precession and its critical radius: $r_c = c / \omega_m$. Where, $\gamma_p = 4.257 \times 10^7$ (Hz/T) is the gyromagnetic ratio of proto.

Note: $e = 1.602 \times 10^{-19}$ (C), $\rho_c = 1 \times 10^{-15}$ m ($\omega_s = 3 \times 10^{23}$ r/s), The strongest interaction happens at $R = \rho_c + b = 1.0009194 \times 10^{-15}$ m. At that place $\gamma_s(R) = -23.3363$, $v_s(R) = 2.9972 \times 10^8$ m/s are definite. If $r_c = 0.499 \times 10^{-15}$ m ($\omega_m = 6.012 \times 10^{23}$ r/s), then $\omega_m' = \omega_m - \omega_s = 3.012 \times 10^{23}$ r/s, $r_c' = 0.996 \times 10^{-15}$ m, $\gamma_m(R) = -[1 - (r_c'/R)^2]^{-1/2} = -10.01$, $v_m(R) = cr_c'/R = 2.988 \times 10^8$ m/s. The magnetic field passing through every proton is: $B = e\gamma_s(R)\gamma_m(R)[v_s(R) + v_m(R)]\mu_0/(4\pi R^2) = 2.2563 \times 10^{15}$ T, which can create the precession of proton with angular velocity of $\omega_m = 2\pi\gamma_p B = 6.035 \times 10^{23}$ r/s, corresponding critical radius is $r_{cc} = c/\omega_m = 0.4971 \times 10^{-15}$ m. That means $r_c = 0.499$ fm can not self-sustain, It will be decreased to 0.4971 fm. As it is decreased to [0.49899063, 0.49899062, 0.49899061] fm, the system parameters are shown in table 3.2.

Table 3.2: The stable self-sustain state of two-proton system with strong interaction

$\gamma_s\gamma_m$	F/F''	B	r_c'	r_c set	r_c create
235.0	468.6	2.247727e+015	9.95971e-016	4.9899061e-016	4.989926e-016
235.0	468.6	2.247736e+015	9.95971e-016	4.9899062e-016	4.989906e-016
235.0	468.6	2.247745e+015	9.95971e-016	4.9899063e-016	4.989886e-016

This means $r_c = 0.4989906(2)$ fm can keep the two protons system self-sustain, as given by the middle row of table 3.2. And this self-sustain state is stable. That means as something makes r_c be changed from $r_c = 0.4989906(2)$ fm, the system can make it return, as shown in table 3.2 (The upper and lower rows). By the way, we always use the three rows table to give the stable self-sustain state in our works. We hope readers can follow it. If the two protons are not shift in lab, then $u_s = 0$, $u_m' = -c\rho_c/R$. The interaction between two protons is following:

$$F_R = F_R'' \gamma_s(R)\gamma_m(R)(1 - v_s(R)u_s/c^2)(1 - v_m(R)u_m'/c^2)$$

$$= F_R'' 235(1 - \rho_c r_c'/R^2) = 468.6 F_R'' = -468.6 ke^2 / R^2$$

It is attraction of 468.6 times stronger than the electrostatic force, and appears at $R = \rho_c + b$ only. This is the so-called strong interaction between two protons and is given in table 3.2 by the term of F/F''. However, the two-proton system cannot be without shift in lab frame. We talk it is just as a foundation of following discuss.

c) Strong interaction between more protons

Consider four protons distribute at the vertices of a square with side length of $R = \rho_c + b = 1.9194$ fm. After longitudinal relaxation, the spin axis and magnetic precession axis of every proton are coincided, and they are antiparallel to the axes of two adjacent protons as shown in Fig.3.3.

Thus, the magnetic field passing through every proton is as following:

$$B = 2\gamma_s(R)\gamma_m(R)e[v_s(R) + v_m(R)]\mu_0/(4\pi R^2) - \gamma_s(\sqrt{2}R)\gamma_m(\sqrt{2}R)e[v_s(\sqrt{2}R) + v_m(\sqrt{2}R)]\mu_0/(8\pi R^2)$$

The critical radius of magnetic precession, which can hold the system stable self-sustaining, is $r_c = 0.4953731 \times 10^{-15}$ m. The stable self-sustain state is given in table 3.3.

Table 3.3: The stable self-sustain state of 4-proton system with strong interaction

$\gamma_s\gamma_m$	F/F''	B	r_c'	r_c set	r_c create
119.5	236.7	2.264148e+015	9.8166229e-016	4.9537315e-016	4.953736e-016
119.5	236.7	2.264150e+015	9.8166233e-016	4.9537316e-016	4.953731e-016
119.5	236.7	2.264153e+015	9.8166237e-016	4.9537317e-016	4.953726e-016

If only take $B = 2\gamma_s(R)\gamma_m(R)e[v_s(R) + v_m(R)]\mu_0 / (4\pi R^2)$, that means neglect the effect of diagonal proton. The stable self-sustain state is given in table 3.4, which is almost the same as table 3.3

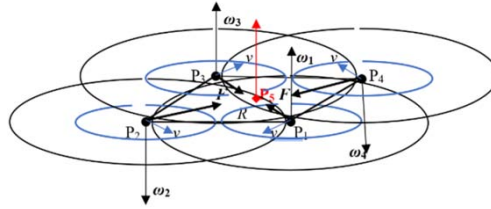


Fig. 3.3: Strong interaction in 4/5-proton system

$\gamma_s\gamma_m$	F/F''	B	r_c'	r_c set	r_c create
119.2	236.0	2.264276e+015	9.8155336e-016	4.9534541e-016	4.953456e-016
119.2	236.0	2.264278e+015	9.8155340e-016	4.9534542e-016	4.953451e-016
119.2	236.0	2.264281e+015	9.8155344e-016	4.9534543e-016	4.953446e-016

Fig. 3.4: The stable self-sustain state of even-proton system with strong interaction

This means that for the multi-proton system distributed in polygon, only the two adjacent protons gives the strong interaction. Thus, we get the force acted on every proton of multi-proton system is as follows

For the proton in 4-proton system $F = 2\sin(\pi/4) \times 236F'' = -334ke^2/R^2$

For the proton in 6-proton system $F = 2\sin(\pi/6) \times 236F'' = -236ke^2/R^2$

For the proton in 8-proton system $F = 2\sin(\pi/8) \times 236F'' = -181ke^2/R^2$

This force is pointed to the center of polygon, which holds the even-proton system stable.

If there is another proton (P_o) located at the center of this polygon, the resultant force exerted by the even protons on P_o is zero. The magnetic field at the center of polygon is zero, so there isn't magnetic precession for P_o . It is only spinning so the force exerted on other even protons is as follows:

For 5-proton system: $F_o = -2\gamma_s(\frac{\sqrt{2}R}{2})ke^2/R^2 = -2.828 ke^2/R^2$ attraction,

For 7-proton system: $F_o = -\gamma_s(R)ke^2/R^2 = 23.3363 ke^2/R^2$ repulsion

For 9-proton system: $F_o = -\gamma_s(\frac{R/2}{\sin(\pi/8)})ke^2/R^2 = 1.5538 ke^2/R^2$ repulsion

For the nuclei with even protons, the magnetic field and angular momentum are cancelled to each other, so there is no spin angular momentum and magnetic moment. And the nuclei with odd protons have only one proton's spin angular momentum and magnetic moment. This conclusion is confirmed by both classical theory and quantum theory. Now we have given its relativistic essence.

d) Sub-strong interaction between protons

As mentioned above, when $R = \rho_c + b > 2r_c$, so that the distance (R) between two protons is greater than both ρ_c and $r_c' = \rho_c \gamma / (\rho_c - r_c)$, the interaction between two protons is strong attraction. However, as $R = \rho_c + b$ is less than r_c , so that the magnetic field passing through every proton is in the same direction as its spin axis, and so that the precession axis of every proton is anti-parallel to its spin axis as shown in Fig.3.4.. In other words, the rotating direction of precession is opposite against that of spin. Thus, relative to spin frame A' the angular velocity of precession frame is $\omega_m' = \omega_s + \omega_m$ i.e. $r_c' = \rho_c \gamma / (r_c + \rho_c)$. And no matter how much is $r_c (> R)$, the r_c' is always less than $\rho_c < R$. This means the force between the two protons is attraction too and can be denoted by following equation as well

$$F_R = F_R'' \gamma_s(R) \gamma_m(R) (1 - v_s(R)u_s/c^2) (1 - v_m(R)u_m'/c^2)$$

PART 4 .NEUTRON AND WEAK INTERACTION

a) The Construction of Neutron

Modern quark theory proposed that the proton is consisted of u-d-u three quarks; neutron is consisted of d-u-d quarks, where u quark carries +2e/3 charge, d quark carries -e/3 charge. However, now we know the charge distribution in proton as shown in Fig. 4.1(a). There is not any negative charge in proton. This means there is not d quark in proton, and proton is not consisted by u-d-u quarks.

From Fig.4.1 (a) we know that the charge density at 0.25 fm is twice of that at 0.75 fm. That means the proton is consisted of three same charged particles, everyone carries +e/3 charge, we call it q quark. And the q quark at 0.75 fm can move from 0.3fm to 1.5fm, that is caused by the measurement. As without measurement, this quark will go back to its original place of 0.3fm, and the three q quarks forms the charge distribution like the part inside 0.3 fm of Fig.4.1 (b). In other words, the part inside 0.3 fm of neutron is just a proton, and the negative charge in neutron must be given by an electron, because the neutron is electricity neutral. It is well known that the neutron can easily decay to proton + electron and neutrino, that is the proof of neutron is consisted of an electron plus a proton.

Now we propose: "the neutron is consisted of a proton and an electron, which is separated from proton by (0.4~1.5)fm". We take it to be $R=0.8 \times 10^{-15}m$ to discuss, and this is the difference from hydrogen atom. In hydrogen atom the distance between proton and electron is in the level of $10^{-10}m$, which is far greater than the spin critical radius of both proton ($\rho_{cp}=10^{-15}m$, i.e. fm) and electron ($\rho_{ce}=10^{-18}m$, i.e. am). Outside the spin critical cylinders, the proton and electron attract to each other and create a rotation around their mass center called system precession with the angular velocity ω_g and critical radius of $l_c=c/\omega_g=7 \times 10^{-9}m$ (we use l to denote the radial of system precession to distinguish from spin (ρ) and magnetic precession r).

However, for neutron the distance between proton and electron is $R=0.8 \times 10^{-15}m$, which is less than $\rho_{cp}=10^{-15}m$. If the critical radius of system precession $l_c > R$, the proton repels electron, system precession can't create. If $l_c < R$ the proton attracts electron, but the mass of electron becomes to negative, since it is outside critical cylinder (OCC) of system precession. Attraction acts on minus mass, the acceleration is centrifugal, the system precession can't create as well. Without system precession, $R=0.8 \times 10^{-15}m < \rho_{cp}=10^{-15}m$, the proton repels the electron with plus mass, the electron will go away. The state can't be stable, the neutron can not exist. However, as the critical cylinder of system precession pass through the charge ball of electron, so that its OCC part suffered from attraction and with minus mass but its ICC part suffered from repulsion and with plus mass. And only as the resultant force is repulsion and the resultant mass is negative, the acceleration of electron is centripetal, the system precession can create and the proton-electron system can be stable, the neutron can exist, as shown in Fig. 4.2.

Now let us give the detail, based on thinking the charge of both proton and electron is uniformly distributed in a ball with radius of $b \approx 1 \times 10^{-18}m$, although they are consisted of three quarks.

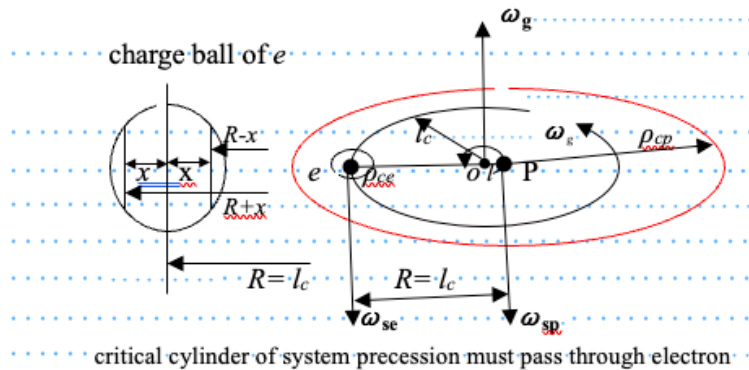


Fig. 4.2: The construction of neutron

Now, let us consider the possibility of this state. Since the critical cylinder of l_c pass through the charge ball of electron, the magnetic field in OCC is opposite against that in ICC, so the magnetic precession of electron can be neglected. On the other hand the critical radius of proton's magnetic precession is on the level of $10^{-13}m$, which is far greater than both ρ_{cp} and l_c , and can be neglect as well. There are only spin and system precession two rotations for both proton and electron.

The mass of proton is 1800 times greater than the mass of electron, so the distance from mass center to proton is $l=R/1800=0.4 \times 10^{-18}m$, which is less than the radius of charge ball $b=1 \times 10^{-18}m$. This means the mass

center is almost coincided with the proton, the system precession of electron can be thought around the proton, And the R and l_c have the same origin $O=P$.

First let us consider the situation of $R=l_c$, that means the critical cylinder of l_c , pass through the charge ball of electron from its center. Take lab as A, system precession as A', in A the electron has only spin. Its mass must be distributed in axis symmetry that means the mass m_0 in cross-plate $R-x$ is equal to that in $R+x$. In lab frame they are rotating with tangential velocity of $v(R-x)=c(R-x)/R$ and $v(R+x)=cR/(R+x)$, The mass becomes to

$$m(R-x) = m_0 / \sqrt{1 - (R-x)^2 / R^2} ;$$

$$m(R+x) = -m_0 / \sqrt{1 - R^2 / (R+x)^2} ,$$

Since $R^2 > R^2 - x^2 = (R-x)(R+x)$, i.e., $R/(R+x) > (R-x)/R$,

So $m(R+x) + m(R-x) < 0$, i.e., the resultant mass is negative as $R=l_c$.

As l_c is increased from $l_c=R$ the ICC part, i. e. , the positive mass is increased. As $l_c=R+b$, the total mass is positive. So there must exist l_{c1} : $R < l_{c1} < R+b$, where the resultant mass equals 0. Thus, keep $l_c < l_{c1}$ can keep the resultant mass to be negative.

b) How doe's weak interaction creates

As mentioned above in system precession frame A', both proton and electron are no shift, the force acted on the electron by spinning proton is $F_R' = \gamma_{sp}(R)ke^2/R^2$, Transform it into lab frame A, we have:

$$F_R = \gamma_{gp}(R) \quad F_R'(1 - u_g v_g(R)/c^2) \tag{4.1}$$

Where $\gamma_{gp}(R) = (1 - v_g^2(R)/c^2)^{-1/2}$, u_g is the tangential velocity of electron in lab frame A .and it just is $u_g = v_g(R)$, since the electron is synchronously rotating with the system precession of proton. So the factor $(1 - u_g v_g(R)/c^2) = (1 - v_g^2(R)/c^2) = 1/\gamma_{gp}^2(R)$. Thus, equation (4.1) becomes to,

$$F_R = F_R' / \gamma_{gp}(R), \text{ i.e. } F_R / F_R' = 1/\gamma_{gp}(R-x).$$

We call it second kind CCE and shown in Fig. 3.1: As R is changed from less than l_c to greater than l_c , the force will pass through 0 and change direction. Partly because second kind CCE, partly because the forces acted on the two sides of critical cylinder are cancelled to each other, the force acted on electron by proton is very weak. Now let us calculate the force as $R=l_c$.

The volume of charge ball is: $4\pi b^3/3$

The charge density in charge ball is: $-3e/(4\pi b^3)$

The volume element at $R-x$ is $dV = \pi[b^2 - x^2]dx$

The charge in this dV is

$$-3e/(4\pi b^3) \times \pi[b^2 - x^2]dx = -(3/4)e[b^2 - x^2]dx/b^3$$

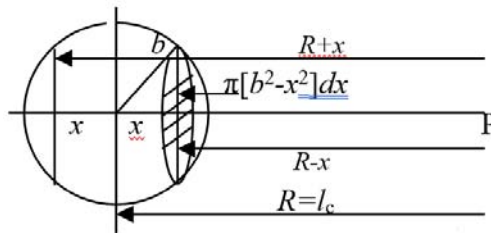


Fig. 4.3: Calculate the resultant force

The total repulsion exerted on electron by proton is:

$$F_i = \int_0^b \left[\frac{\gamma_s(R-x)}{\gamma_g(R-x)} \right] \left[\frac{ke^2}{(R-x)^2} \right] \left[\frac{3(b^2 - x^2)}{4b^3} \right] dx$$

The total attraction exerted on electron by proton is:

$$F_o = \int_0^b \left[\frac{\gamma_s (R+x)}{\gamma_g (R+x)} \right] \left[\frac{ke^2}{(R+x)^2} \right] \left[\frac{3(b^2-x^2)}{4b^3} \right] dx$$

As $R=l_c=0.8\text{fm}$; $b=10^{-18}\text{m}=1\text{am}$ The resultant force is: $F=F_i+F_o=0.002197$ (N), and it is repulsion.

As $R=0.8\text{fm}$ the electrostatic force is $F_c=ke^2/R^2=344.7419$ (N), so $F \approx 6/10^6 F_c$ is very weak repulsion.

This is so-called weak interaction acted on electron (by proton). They found this repulsion, and could not think it came from proton, constrained by Coulomb's law. And though it came from lepton.

As l_c is decreased from $R=l_c$, the repulsion F_i is decreased and the attraction F_o is increased. There must exist l_{c2} : $R-b < l_{c2} < R$, where resultant force $F=0$. Keep $l_c > l_{c2}$ can keep the resultant force to be repulsion.

Thus, only if $l_{c1} > l_c > l_{c2}$ the system precession can create, the neutron can stably exist. The magnetic resonance therapy just makes l_c to beyond this scope, so that the neutron will decay and epoxide be damaged.

Year 2025

24

c) *The Stable State of Neutron* ($l_{c2} < l_c < l_{c1}$)

For proton: The force exerted on proton by electron is: $F = \frac{\gamma_{se}(R) ke^2}{\gamma_{ge}(l) R^2} = -\frac{ke^2}{R^2}$ where l is the distance from mass

center to proton, In terms of $F = ma = \frac{mv^2}{l} = \frac{mc^2 l}{l_c^2}$ we have $l_c^2 = \frac{mc^2 l}{F}$ As $l = 1.532 \times 10^{-18}\text{m}$, $R = 0.8\text{fm}$ the l_{cp} is

$$0.8\text{fm} \text{ For electron: } F = ma = \frac{mv^2}{R} = \begin{cases} mc^2 R / l_c^2 & R < l_c \\ mc^2 l_c^2 / R^3 & R > l_c \end{cases} \text{ We have } l_c^2 = \begin{cases} mc^2 R / F & R < l_c \\ R^3 F / mc^2 & R > l_c \end{cases}$$

We know the decreased force F but do not know the decreased mass m . Suppose the decreased force $F = aF_r$ ($a < 1$), the decreased mass $m = anm_e$ where $F_r = -ke^2 / R^2$, is the electrostatic force $m_e = 9.09 \times 10^{-31}\text{kg}$ is the rest mass of electron. Thus, we have

$$l_c^2 = \begin{cases} nm_e c^2 R / F_r & R < l_c \\ R^3 F_r / (nm_e c^2) & R > l_c \end{cases} \text{ i.e. : } l_{ce} = \begin{cases} c \sqrt{(m_e n R) / F} & R < l_{ce} \\ \sqrt{F R^3 / (m_e n c^2)} & R > l_{ce} \end{cases}$$

Then, take $F = -ke^2 / R^2$, $m_e = 9.09 \times 10^{-31}\text{kg}$, $R = 0.8\text{fm}$ we get following result:

n	l	ω_p	l_{cp}	l_{cei}	l_{ceo}
3.5170	1.532e-018	3.75e+023	8e-016	7.9999e-016	8.0001e-016
3.5171	1.532e-018	3.75e+023	8e-016	8e-016	8e-016
3.5172	1.532e-018	3.75e+023	8e-016	8.0001e-016	7.9999e-016

That means as $n=3.5171$ $l_{cp} = l_{cei} = l_{ceo} = 0.8 \times 10^{-15}\text{m} = R$, that is a stable self-sustain state

Different deep of critical cylinder passing though the charge ball, corresponding different n , the stable state is different. As $n=2.3447$ $R=1.2\text{fm}$ the critical radius of stable state is $l_{cp} = l_{cei} = l_{ceo} = 1.2 \times 10^{-15}\text{m}$ as shown in follows:

Global Journal of Research in Engineering (J) XXV Issue I Version I

n	l	ω_p	l_{cp}	l_{cei}	l_{ceo}
2.3444	1.532e-018	2.5e+023	1.2e-015	1.1999e-015	1.2001e-015
2.3447	1.532e-018	2.5e+023	1.2e-015	1.2e-015	1.2e-015
2.3450	1.532e-018	2.5e+023	1.2e-015	1.2001e-015	1.1999e-015

This is why the negative charge can distribute in $[0.5\sim 1.5] \times 10^{-15}m$ so wide area in Fig. 4. 1.

d) *The Strong Interaction between Neutrons*

Knowing the neutron is consisted of a proton plus an electron, we know the strong interaction between neutrons just is the strong interaction between their protons. and the influence of the electron to other neutrons can be neglected. Consider four-neutron system, their protons distribute at the vertices of a square with side length of $R=\rho_{cp}+b$, as shown in Fig.4.4. Every proton locates Outside Critical Cylinders of both spin and system precession of the other protons, so the four protons attract to each other. The critical radius of magnetic precession of every proton must be greater than $R=\rho_{cp}+b$ for both r_c (relative to lab) and r'_c (relative to its spin), which is kept by electron's magnetic field and enough big of r_c .

Take lab as A, spin of P_1 is A' the magnetic precession of P_1 as A'', the system precession of P_1 -e₁ as A'''

Then, in A''' P_1 is really at rest, the force acted by P_1 on other proton is the real electrostatic force $F''' = -ke^2/R^2$. Transform it into A'', then A', then A, we have:

$$F_R = F_R''' \gamma_s(R) \gamma_m(R) \gamma_g(R) (1 - v_s(R)u_s/c^2) (1 - v_m(R)u_m'/c^2) (1 - v_g(R)u_g''/c^2)$$

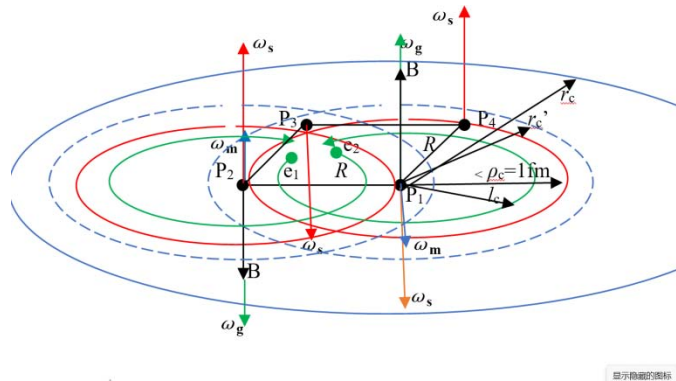


Fig. 4.4: The four-neutron system

The magnetic field passing through every neutron's proton is as follows

$$B_n = 2\gamma_s(R)\gamma_m(R)\gamma_g(R)e[v_s(R) + v_m(R) - v_g(R)]\mu_0/(4\pi R^2) - ec\mu_0/(4\pi l_c^2)$$

Where the last term come from: $-\gamma_{se}(l_c)\gamma_g(0)ev_{se}(l_c)\mu_0/(4\pi l_c^2)$, that is the orbit magnetic field of electron

The stable self-sustaining state is as follows:

$\gamma_s\gamma_m\gamma_g$	B	l_c'	r_c'	r_c set	r_c create
35.4749	3.656e+014	5.1974e-016	1.484e-015	3.0678e-015	3.0680e-015
35.4753	3.656e+014	5.1974e-016	1.484e-015	3.0679e-015	3.0679e-015
35.4757	3.656e+014	5.1974e-016	1.484e-015	3.0680e-015	3.0679e-015

As the four proton are no shift in lab, $u_s=0$, $u_m'=-c\rho_c/R$, $u_g''=c(\rho_c+r_c)/(1+r_c\rho_c)$,

The attraction between two neutrons is as follows:

$$F_R = F_R''' \gamma_s(R) \gamma_m(R) \gamma_g(R) (1 - v_s(R)u_s/c^2) (1 - v_m(R)u_m'/c^2) (1 - v_g(R)u_g''/c^2)$$

$$F_R = 35.5F_R'''(1 + \rho_c / r_c')(1 - \frac{l_c'}{R}(\frac{r_c' + \rho_c}{1 + \rho_c r_c'})) = 29F_R'''$$

Thus, we get the force acted on every neutron's proton of multi-neutron system is as follows

For the proton in 4-neutron system $F = 2\sin(\pi/4) \times 29F'' = -41ke^2/R^2$

For the proton in 6-neutron system $F = 2\sin(\pi/6) \times 29F'' = -29ke^2/R^2$

For the proton in 8-neutron system $F = 2\sin(\pi/8) \times 29F'' = -22ke^2/R^2$

This is the strong interaction between multi neutrons. Obviously, it is not so strong as that between multi protons. However, the strong interaction between, say, the system consisted of two protons and two neutrons is in the same level as that of four protons. Following is the stable self-sustain state with strong interaction for 2-proton2-neutron system.

γ_p	γ_n	r_{cp}'	$r_{cp}(\text{set})$	$r_{cp}(\text{create})$	r_{cn}'	r_{cn}	l_c'
117.6	153.5	9.81e-16	4.95209355e-16	4.95212e-16	1.0157e-15	5.03892e-16	4.475e-16
117.6	153.5	9.81e-16	4.95209356e-16	4.95207e-16	1.0157e-15	5.03892e-16	4.475e-16
117.6	153.5	9.81e-16	4.95209357e-16	4.95204e-16	1.0157e-15	5.03891e-16	4.475e-16

As the four protons are no shift in lab frame, the force exerted on every proton by every neutron is as follows:

$$F_p = 153.5F_R''' \left(1 + \left(\frac{\rho_c}{R} \right) \left(r_{cp}' \frac{1}{R} \right) \right) = 304F_R'''$$

The force exerted on every neutron by every proton is as follows:

$$F_n = 117.6F_R'''(1 + \rho_c/r_{cn})(1 - \frac{l_c'}{R}(\frac{r_{cn}' + \rho_c}{1 + \rho_c r_{cn}})) = 127F_R'''$$

And their stable self-sustain state with sub-strong interaction is as follows

γ_p	γ_n	r_{cp}'	$r_{cp} \text{ set}$	$r_{cp} \text{ create}$	r_{cn}'	r_{cn}	l_c'
49.0	89.4	8.802e-16	7.34920e-15	7.34923e-15	9.64518e-16	2.71829e-14	4.69016e-15
49.0	89.4	8.802e-16	7.34922e-15	7.34922e-15	9.64518e-16	2.71830e-14	4.69016e-15
49.0	89.4	8.802e-16	7.34924e-15	7.34921e-15	9.64518e-16	2.71830e-14	4.69016e-15

As the four protons are no shift in lab frame, the force exerted on every proton by every neutron is as follows:

$$F_p = 89.4 F_R'''(1 - (\rho_c/R)(r_{cp}'/R)) = 10.7 F_R'''$$

The force exerted on every neutron by every proton is as follows:

$$F_n = 49 F_R'''(1 - (\rho_c/R)(r_{cn}'/R))(1 + (l_c'/R)) = 3 F_R'''$$

Thus, we know the force acted on neutron is less than that on proton, The MRT just make neutron decay to damage the epoxide to treat cancer. We will give the detail in another paper.

PART 5. HOW DOES QUANTUM PROPERTY CREATE

a) Quantum Property Comes from the CCE of Field Energy

Now, let us discuss the critical cylinder effect (CCE) of Energy and Mass (E-M) of spinning charged particle, based on thinking its charge q to be uniformly distributed in a charge ball of radius b , even though the particle may possess complex internal structure.

For the spinning charged particle, take the laboratory as reference frame A and the spin of the particle as reference frame A' . In frame A' , the particle is indeed at rest, and its electric field is the true electrostatic field. The value of this electrostatic field at a distance r from the center of charge ball is:

$$E_r' = \begin{cases} -kqr/b^3, & r < b \\ -kq/r^2, & r > b \end{cases} \quad (5.1)$$

where $k = 1/(4\pi\epsilon_0)$.

The field energy w' at that point is:

$$w'(r) = (\epsilon_0/2)E_r'^2 = \begin{cases} (\epsilon_0/2)k^2q^2r^2/b^6 & r < b \\ (\epsilon_0/2)k^2q^2/r^4 & r > b \end{cases} = \begin{cases} (1/8\pi)kq^2r^2/b^6 & r < b \\ (1/8\pi)kq^2/r^4 & r > b \end{cases} \quad (5.2)$$

The total field energy of the charged particle in its spinning reference frame is obtained by integrating the energy density $w'(r)$ over the entire three-dimensional space. When this integral is calculated in the (r, φ, θ) sphere coordinate system, the energy inside charge ball, W_i' , is:

$$W_i' = \frac{\epsilon_0 k^2 q^2}{2b^6} \int_0^{2\pi} d\varphi \int_0^{\pi/2} \sin\theta d\theta \int_b^\infty 2r^4 dr = \frac{kq^2}{10b} \# \quad (5.3)$$

The energy outside charge ball, W_o' , is:

$$W_o' = \frac{\epsilon_0 k^2 q^2}{2} \int_0^{2\pi} d\varphi \int_0^{\pi/2} \sin\theta d\theta \int_b^\infty \frac{2}{r^2} dr = \frac{kq^2}{2b} \# \quad (5.4)$$

Similarly, the energy outside the ball with radius of a ($a > b$), W_{ao}' , is:

$$W_{ao}' = \frac{kq^2}{2a} \# \quad (5.5)$$

If $a = 1000b$, then $W_{ao}' = 0.001W_o'$. This indicates that 99.9% of the energy outside the charged ball is contained within a sphere of radius a equals $1000b$. Conversely, if $a=2b$, then $W_{ao}' = W_o'/2$, meaning that half of the energy outside the charged ball is located within the spherical shell defined by $b < r < 2b$. The total field energy in the spinning frame, denoted as W' is given by:

$$W' = W_i' + W_o' = \frac{1.2kq^2}{2b} \# \quad (5.6)$$

For a proton, the charge q is $1.602 \times 10^{-19} \text{C}$. If the radius b is $0.9194 \times 10^{-18} \text{m}$, then the total field energy W' is $1.5053 \times 10^{-10} \text{J}$. This energy corresponds to the rest mass of $m' = \frac{W'}{c^2} = 1.67252 \times 10^{-27} \text{Kg}$, which just is the rest mass of a proton. This leads to the idea that "mass arises from its field energy." This result denotes that the particle's field energy in the spinning frame is a single, definite value, lacking quantum property. Thus, we can think the charge of proton ($e = 1.602 \times 10^{-19} \text{C}$) is uniformly distributed in a ball with radius of $b = 0.6ke^2/W' = 0.9194 \times 10^{-18} \text{m}$, that has been used in part 3 and 4.

In terms of energy-momentum transformation:

$$w = \gamma(\rho)(w' + v(\rho)p_s') \# \quad (5.7)$$

Since the momentum in the spinning frame is zero ($p'_s=0$), Consequently, the field energy at $r = \sqrt{\rho^2 + z^2}$ from the center of the charged ball in the laboratory frame A can be expressed as follows:

$$w(\rho) = \begin{cases} \frac{\gamma(\rho)\left(\frac{\epsilon_0}{2}\right)k^2q^2r^2}{b^6} & r < b \\ \frac{\gamma(\rho)\left(\frac{\epsilon_0}{2}\right)k^2q^2}{r^4} & r > b \end{cases} \quad \# \quad (5.8)$$

where

$$\gamma(\rho) = \begin{cases} \frac{1}{\sqrt{1-\left(\frac{\rho}{\rho_c}\right)^2}}, \rho < \rho_c \\ -\frac{1}{\sqrt{1-\left(\frac{\rho_c}{\rho}\right)^2}}, \rho > \rho_c \end{cases}$$

The total field energy of a spinning charged particle in the laboratory frame is obtained by integrating the energy at each point: $w(\rho)$, over the entire three-dimensional space. However, since $w(\rho)$ depends on $\gamma(\rho)$ and the expression of $\gamma(\rho)$ in ICC differs that in OCC, this integration must be divided into four distinct parts:

- (A) W_1 for the region where $b < \rho < \rho_c$
- (B) W_2 for the region where $\rho_c < \rho < \infty$
- (C) W_3 for the region where $\rho < b, z > \sqrt{b^2 - \rho^2}$
- (D) W_4 for the region where $\rho < b, z < \sqrt{b^2 - \rho^2}$

These regions are illustrated in Figure 5.1.

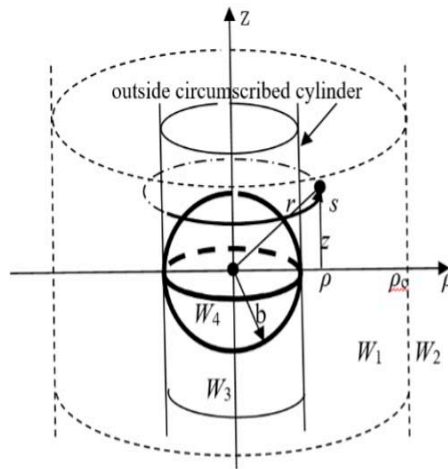


Fig. 5.1: Charge Ball and Critical Cylinder

For the location of $b < \rho < \rho_c$, the energy W_1 is given by

$$W_1 = \frac{\epsilon_0 k^2 q^2}{2} \int_b^{\rho_c} \frac{d\rho}{\sqrt{1-\rho^2/\rho_c^2}} d\rho \int_0^{2\pi\rho} ds \int_0^\infty \frac{2dz}{(\rho^2+z^2)^2} \quad (5.9)$$

Note that: $\int_0^\infty \frac{dz}{(\rho^2+z^2)^2} = \left[\frac{z}{2\rho^2(\rho^2+z^2)} + \frac{\arctan\left(\frac{z}{\rho}\right)}{2\rho^3} \right]_0^\infty$

$$= \frac{\pi\left(n \pm \frac{1}{2}\right)}{2\rho^3}, n = 0,1,2, \dots$$

Thus,

$$W_1 = \frac{kq^2}{4} \pi \left(n \pm \frac{1}{2} \right) \int_b^{\rho_c} \frac{\rho_c d\rho}{\rho^2 \sqrt{\rho_c^2 - \rho^2}}$$

$$= \frac{kq^2 \pi}{2b} \left(n \pm \frac{1}{2} \right) \sqrt{1 - \frac{b^2}{\rho_c^2}}, n = 0, 1, 2, \dots \# \quad (5.10)$$

For the location of OCC where $\rho_c < \rho < \infty$, we have:

$$\begin{aligned} W_2 &= \frac{\epsilon_0 k^2 q^2}{2} \int_0^{2\pi\rho} ds \int_{\rho_c}^{\infty} -(1 - \rho_c^2/\rho^2)^{-1/2} d\rho \int_0^{\infty} \frac{2dz}{(\rho^2 + z^2)^2} \\ &= \frac{kq^2}{4} \pi \left(n \pm \frac{1}{2} \right) \int_{\rho_c}^{\infty} \frac{-d\rho}{\rho \sqrt{\rho^2 - \rho_c^2}} = -\frac{kq^2 \pi \left(n \pm \frac{1}{2} \right)}{4} \left(\frac{\arccos(\rho_c/\rho)}{\rho_c} \right) \Big|_{\rho_c}^{\infty} \\ W_2 &= -\frac{kq^2 \pi^2}{4\rho_c} \left(n \pm \frac{1}{2} \right) \left(m \pm \frac{1}{2} \right), \quad n = 0, 1, 2, \dots, m = 0, 1, 2, \dots \# \end{aligned} \quad (5.11)$$

The total energy outside the circumscribed cylinder of the charge ball in the laboratory frame A is:

$$\begin{aligned} W_1 + W_2 &= \frac{kq^2 \pi}{2b} \left\{ \sqrt{1 - \frac{b^2}{\rho_c^2}} - \frac{b\pi}{\rho_c} \left(m \pm \frac{1}{2} \right) \right\} \left(n \pm \frac{1}{2} \right), \\ n &= 0, 1, 2, \dots, m = 0, 1, 2, \dots \# \end{aligned} \quad (5.12)$$

This implies that the energy of a spinning charged particle in the laboratory frame has multiple values, leading to the mass also having multiple values. This characteristic is referred to as the quantum property of a spinning charged particle. Clearly, this quantum property arises from the critical cylinder effect (CCE). The factor $(n \pm 1/2)$, $n=0, 1, 2, \dots$ represents both the principal quantum number n and the spin quantum number $s = \pm 1/2$. Meanwhile, the factor $(m \pm 1/2)$, $m=0, 1, 2, \dots$, accounts for the Zeeman splitting.

Similarly, the energy within the circumscribed cylinder of the charge ball, but outside the charge ball itself, is described by the following expression.

$$W_3 = \frac{\epsilon_0 k^2 q^2}{2} \int_0^b \gamma(\rho) d\rho \int_0^{2\pi\rho} ds \int_{\sqrt{b^2 - \rho^2}}^{\infty} \frac{2dz}{(\rho^2 + z^2)^2} \quad (5.13)$$

Unfortunately, this expression does not have an analytic solution. However, it must be multivalued because it includes the integral of $\int_{\sqrt{b^2 - \rho^2}}^{\infty} \frac{2dz}{(\rho^2 + z^2)^2}$:

The total energy within the charge ball is given by the following expression, which lacks an analytic solution:

$$W_4 = \frac{\epsilon_0 k^2 q^2}{2b^6} \int_0^b \frac{2d\rho}{\sqrt{1 - \frac{\rho^2}{\rho_c^2}}} d\rho \int_0^{2\pi\rho} ds \int_0^{(b^2 - \rho^2)^{\frac{1}{2}}} (\rho^2 + z^2) dz \# \quad (5.14)$$

In addition to spin, charged particles can exhibit other types of rotation, such as magnetic precession and system precession. Each type of rotation has its own CCE, which can result in the energy having multiple values. These variations in energy are the sources of what are known as the magnetic and angular quantum numbers. The presence of these quantum numbers reflects the complex rotational dynamics of charged particles, contributing to their unique quantum properties.

b) The Field Energy and Mass of Proton

For proton, where $\rho_c = 10^{-15} \text{m} \gg b = 0.9194 \times 10^{-18} \text{m}$, neglecting b/ρ_c , following Eq. (5.12)

$$W_1 + W_2 = \frac{kq^2 \pi}{2b} \left\{ \sqrt{1 - \frac{b^2}{\rho_c^2}} - \frac{b\pi}{\rho_c} \left(m \pm \frac{1}{2} \right) \right\} \left(n \pm \frac{1}{2} \right)$$

can be expressed as follows:

$$W_1 + W_2 = \frac{kq^2 \pi}{2b} \left(n \pm \frac{1}{2} \right), n = 0, 1, 2, \dots,$$

The difference between $n=1$ and $n=0$ is called quantum interval, and is $\Delta W = \frac{kq^2 \pi}{2b}$

Substituting $b=0.9194 \times 10^{-18} \text{m}$, $K=8.988 \times 10^9$, $q=1.602 \times 10^{-19} \text{C}$ the quantum interval of energy for proton is as follows: $\Delta W = \frac{kq^2 \pi}{2b} = 1.9705 \times 10^{-10} \text{ (J)}$

Note that $\rho_c = c/\omega_s = 10^{-15} \text{m}$ means the spin angular velocity is $\omega_s = c/\rho_c = 3 \times 10^{23} \text{ (r/s)}$, we have.

$$\Delta W / \omega_s = 6.5683 \times 10^{-34} \text{ (Js)}$$

This indicates that the energy quantum interval ΔW is proportional to ω_s , with a proportionality constant of $6.5683 \times 10^{-34} \text{ (Js)}$, which corresponds to Planck's constant: $h = 6.6256 \times 10^{-34} \text{ (Js)}$.

The critical radius associated with the spin of a proton is approximately $\rho_c = 10^{-15} \text{ m}$, which is thousand times larger than b . As result, over 99.9% of the proton's energy or mass is contained within ICC. This significant concentration allows us to neglect the mass present in the OCC and the multivalued property given by $m=0, 1, 2, 3, \dots$

c) *The Energy-Mass of electron and Dark Mass*

In contrast, the critical radius of an electron's spin is closely aligned with the charge ball's radius. This proximity necessitates considering the field energy of the electron in both ICC and OCC. The total energy in the OCC is not only multivalued but also negative, allowing it to cancel the positive energy in the ICC. Assuming the radius of the electron's charge ball is the same as that of the proton, due to their identical absolute charge, the critical radius for the electron's spin should be $\rho_c = 1.16 \times 10^{-18} \text{ m}$.

In this scenario, for the state characterized by $n=0$, $s=1/2$, and take $(m \pm 1/2)$ to be $1/2$, the total energy in the OCC is:

$$W_2 = -\frac{kq^2 \pi^2}{16\rho_c} = -12.266 * 10^{-11} \text{ (J)}$$

The energy outside circumscribed cylinder of charge ball but within critical cylinder is:

$$W_1 = \frac{kq^2 \pi}{2b} \frac{1}{4} \sqrt{1 - b^2/\rho_c^2} = 5.91145 * 10^{-11} \text{ (J)}$$

The energy within the charge ball can be determined through numerical integration,

$$W_4 = \frac{\epsilon_0 k^2 q^2}{2b^6} \int_0^b \frac{2d\rho}{\sqrt{1-\rho^2/\rho_c^2}} d\rho \int_0^{2\pi\rho} ds \int_0^{(b^2-\rho^2)^{1/2}} (\rho^2 + z^2) dz = 3.01 * 10^{-11} \text{ (J)}$$

Using numerical integration, the energy within the circumscribed cylinder of the charge ball but outside the charge ball itself is calculated as follows:

$$W_3 = \frac{\epsilon_0 k^2 q^2}{2} \int_0^b \gamma(\rho) d\rho \int_0^{2\pi\rho} ds \int_{\sqrt{b^2-\rho^2}}^\infty \frac{2dz}{(\rho^2 + z^2)^2} = 3.35 * 10^{-11} \text{ (J)}$$

Thus, the total energy of a spinning electron in the laboratory frame for the state characterized by $m=0$, $n=0$, $s=1/2$ is as follows:

$$W = W_1 + W_2 + W_3 + W_4 = 8.2 \times 10^{-14} \text{ J.}$$

This energy corresponds to a mass of $m = W/c^2 = 9.1 \times 10^{-31} \text{ Kg}$ that is well known electron's mass.

In spin frame, the mass of an electron is calculated as $0.6ke^2/b = 1.6725 \times 10^{-27} \text{ Kg}$, However, in the laboratory frame, it is $9.1 \times 10^{-31} \text{ Kg}$. The difference of $1.6716 \times 10^{-27} \text{ Kg}$ is referred to as "dark mass," which can be partially "relit" by other types of rotations, such as magnetic precession or system precession.

This understanding not only reveals the source of quantum properties but also elucidates the origins of mass and dark mass. In the laboratory frame, mass is distributed on either side of the critical cylinder with opposite signs, effectively canceling each other out. The so-called rest mass of charged particles in the laboratory frame is merely the remainder after this cancellation, rather than the true rest mass in the spin frame. Therefore, what is termed "dark matter" is simply the portion of mass that is canceled out in the laboratory frame; it exists in spinning frame but remains undetectable in the laboratory frame.

It should be pointed out that the dark matter mentioned here is not the same thing as that mentioned by the academic community.

According to Newton's law, the gravitational pull of a galaxy with mass M on a planet with mass m is $F=GMm/R^2$. The centripetal acceleration produced by the planet under this gravitational pull is $a=v^2/R$, where v is the tangential velocity of the planet. According to $F=ma$, $v=(GM/R)^{1/2}$ can be obtained, that is, the farther the distance, the slower the velocity.

However, when observing the rotation of spiral galaxies, it is found that the tangential velocity of the planets at the edge of the galaxy increases with distance, and according to $v=(GM/R)^{1/2}$, scholars believe that this indicates that the mass M increases with distance, so they propose that there is a kind of "dark matter" that we cannot see around the galaxy. This material exerts an additional gravitational pull on the planets at the edge of the galaxy, causing them to rotate faster.

We don't think such dark matter exists. The original reason of the rotation speed of the planet does not decrease but rises with distance, not the existence of dark matter, but the relativistic effect of rotation. To simplify the discussion, let's consider the force of a central planet with mass M on a marginal planet with mass m , when the central planet spins with ρ_c and rotates with the marginal planet around their mass center with the critical radius of lc . Take lab as frame A, system precession as A', the spin of central planet as A'', then in A'' the force acted by M on m is $F''=GMm/R^2$, but in lab frame it becomes follows

$$F = \gamma_s(R)/\gamma_g(R) \frac{GMm}{R^2} = \frac{\sqrt{1 - R^2/l_c^2} M Gm}{\sqrt{1 - R^2/\rho_c^2} R^2}$$

where R is the distance between two planets and when it is far less than lc , this equation can be simplified as:

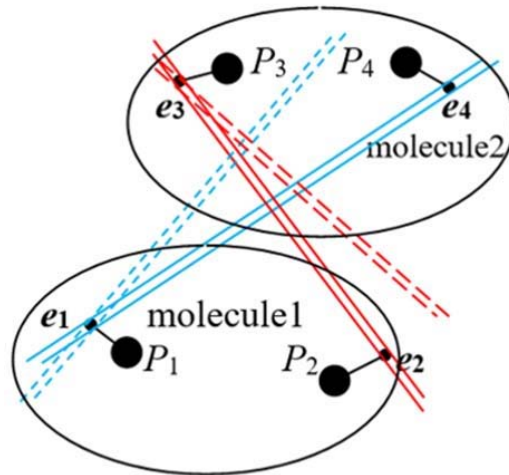
$$F = \gamma_s(R) \frac{GMm}{R^2} = \frac{M}{\sqrt{1 - R^2/\rho_c^2}} \frac{Gm}{R^2} \dots\dots\dots v=(\gamma_s GM/R)^{1/2}$$

When R increases and approaches ρ_c , M does not change but the Lorentz factor γ_s increases, causing the rotational velocity of the marginal planets to increase. This is relativistic effect but not dark matter.

d) *How Does Gravitation Create*

Mass comes the field energy; the gravitation must be related to electromagnetic force. It comes from the CCE of electron's spin, i.e.: the electron attracts the other electron inside critical cylinder and repels the electron outside critical cylinder.





As the critical cylinder of e_1 including e_4
 e_1 attract both e_4 and P_4
 As the critical cylinder of e_3 including e_2
 e_3 attract both e_2 and P_2

Fig. 5.1: Gravity comes from CCE

Consider the four proton-electron (p-e) pairs located in two molecules as shown in Fig. 5.1 As the spin critical cylinder (SCC) of e_1 doesn't include p_3-e_3 and p_4-e_4 , it attracts p_3p_4 , repels e_3e_4 , the resultant force is $F=0$.

As the SCC of e_1 includes, say, e_4 , it attracts p_3p_4 and e_4 , repels e_3 , the resultant attraction is $F=-2ke^2/R^2$

Similarly, as the spin critical cylinder (SCC) of e_3 includes e_2 , molecule 2 attracts molecule1 with the same $F=-2ke^2/R^2$. These two attractions are the source of gravitation.

The distance between molecules is on the level of $R=10^{-9}$ m, and the critical radius of electron's spin is $\rho_{ce}=10^{-18}$ m, the probability by which the SCC of e_1 includes e_4 is:

$$\pi\rho_{ce}^2/(4\pi R^2)=10^{-36}/(4\times 10^{-18})=0.25\times 10^{-18}.$$

Similarly, the probability by which the SCC of e_3 includes e_2 is the same 0.25×10^{-18} . The probability of these two events happens in the same time is 6.25×10^{-38} . That means the gravitation is only on the 10^{-38} level of electromagnetic interaction, which is known by modern physics.

Obviously, the gravitation is proportional to the number of electrons in a body. And in the natural body the number of electrons is equal to the number of protons (the neutron is consisted of a proton and an electron), so the number of electrons is proportional to the mass of the body. That made Newton thought the gravitation came from mass.

II. CONCLUSION

1. Cancer and cardio- and brain-vascular diseases are top two killers of mankind. MRT can not only treat but also prevent them. Besides, MRT can treat lots of other diseases caused by oxidation. Once it is popularized into every family, the level of health will be increased.
2. The Relativity for Rotational Frames reveals lots of natural laws, which are unknown for modern physics, such as space time exchange, the tangential velocity for OCC is $c^2/(\rho\omega)$, the critical cylindrical effects, which indicate the force will change direction, as the acceptor is changed from ICC to OCC, and is verified by our experiment
3. Strong, weak and gravity are all electromagnetic interaction suffered from different Critical Cylinder Effects (CCE).
4. Only based on relativity for rotational frames the research about both astronomy and basic particles can touch the essence.
5. The quantum property comes from the CCE of field energy The uncertainty of particle world comes from the stochastic direction of donor's spin axis. We open a way to unify the quantum mechanics with relativity.

ACKNOWLEDGEMENTS

A special acknowledgment is due to our Guides and teachers and Dr. C.N. Yang, Dr. H. T. Nieh and Dr. P. Lauterbur in the State University of New York at Stony Brook, and Dr. R. A. Scheuing, Dr. T. C. Fang in the Grumman Aerospace Corporation for their kindly inviting and supporting me to do some research work in the SUNY at Stony Brook. A special acknowledgment is due to Prof. B. Nordenström in Karolinska Medical Institute and Prof. Y. L. Xin in Chinese-Japanese Friendship Hospital for their kindly inviting me to do some research work about Electric-Chemical Therapy of cancer. I wish to thank Prof. S. Zhou and Prof. Y. C. Chi in Chinese-Japanese Friendship Hospital for their kindly helping us to do the cells and animals experiments of MRT. I wish to thank Prof. D. C. Tao in Analogic Corporation and Prof. J. Z. Hoang in Hang Zhou Railroad Central Hospital for their kindly supporting us to do the clinical experiments of MRT. A special hallow is due to the volunteers. At last thanks editorial department of AJBSR and editor Elena Moore for their work in publishing this booklet.

REFERENCES RÉFÉRENCES REFERENCIAS

1. James D. Watson, Molecular Biology of the Gene, W. A. BENJAMIN INC. 1977.
2. Yin Rui, Rotating Lorentz Transformation and Unification of Forces, B.U.A.A. Press, Beijing, 1997.
3. Yin Rui, Unification of Forces According to Relativity for Rotations, H Adronic Journal, Volume 23, Number 5, October 2000, pp. 487-549. (Note: page 497 should be between 492 and 493).
4. C. Møler, THE THEORY OF RELATIVITY, Clarendon Press Oxford 1972.
5. Zhang San-Hui, Physics in University Tzing-Hua University Press 2009.
6. Yin Rui, Yin Ming, Wang Yang: Critical cylindrical Effect and space-time exchange in rotational reference frames of special relativity; World Academy of Science, Engineering and technology (Physical and Mathematical Sciences) Online ISSN 1307 6892.
7. Yin Rui, Yin Ming, Wang Yang: Magnetic Resonance Therapy (MRT) and Relativity America Journal of Biomedical Science & Research 2024, Tissue 5.
8. Yin Rui, Yin Ming, Wang Yang: Magnetic Resonance Therapy (MRT) Treat cardio- and brain-vascular diseases America Journal of Biomedical Science & Research 2024, Tissue 6.

